Available online at www.sciencedirect.com
SCIENCE DIRECT
Tectonophysics 421 (2006) 23–51
TECTONOPHYSICS
www.elsevier.com/locate/tecto

Late Tertiary–Quaternary tectonics of the Southern Apennines (Italy): New evidences from the Tyrrhenian slope

Cesare Caiazzo, Alessandra Ascione *, Aldo Cinque

Dipartimento di Scienze della Terra, Università degli Studi di Napoli "Federico II", Largo S. Marcellino 10, 80138 Napoli, Italy

Received 13 June 2005; received in revised form 22 March 2006; accepted 7 April 2006
Available online 23 June 2006

Abstract

This paper summarises the results of combined structural and geomorphological investigations we carried out in two key areas, in order to obtain new data on the structure and evolution of the Tyrrhenian slope of the southern Apennines. Analysis by a stress inversion method [Angelier, J., 1994. Fault slip analysis and paleostress reconstruction. In: Continental Deformation. P.L. Hancock Ed., Pergamon Press, Oxford, 53–100] of fault slip data from Mesozoic to Quaternary formations allowed the reconstruction of states of stress at different time intervals. By integrating these data with those deriving from the stratigraphic and morphotectonic records, chronology and timing of the sequence of the deformation events was obtained.

The tectonic history of the region can be related to four deformation events. Structures related to the first event, that was dominated by a strike-slip regime with a NW–SE oriented $\sigma 1$ and was active since Mid–Late Miocene, do not significantly affect the present day landscape, as they were strongly displaced and overprinted by subsequent deformation events and/or deleted by erosion. The second and third events, that may be considered as the main responsible for the morphostructural signature of the region, are comparable with the stretching phases recognised offshore and considered to be responsible for the opening and widening of the Tyrrhenian basin. In particular, the second event (with an E–W oriented $\sigma 3$), took place in the Late Miocene/earliest Pliocene and was first dominated by a strike-slip regime, that was also responsible for thrusting and folding. Since Late Pliocene, it was dominated by an extensional regime that created large vertical offsets along N–S to NW–SE trending faults. The third event, that was dominated by extension with a NW–SE oriented $\sigma 3$, started in the Early Pleistocene and was responsible for formation of the horst-and-graben structure with NE–SW trend that characterises the Tyrrhenian margin of the southern Apennines. The fourth deformation event, which is characterised by an extensional regime with a NE–SW trending $\sigma 3$, started in the late Middle Pleistocene and is currently active.

Keywords: Paleostresses; Morphotectonics; Pliocene; Quaternary; Southern Apennines; Italy

1. Introduction

The Southern Apennines (Fig. 1) are a fold-and-thrust belt resulting from the latest interactions between the Adriatic promontory of the African plate and the European plate (Cello et al., 1990; Cello and Mazzoli, 1999). Accretion of the Southern Apennines wedge took place from the Early Miocene to the Early Middle Pleistocene (Amore et al., 1988; Patacca et al., 1990; Patacca and Scandone, 2001) due to deformation of the Adriatic westward subducting margin. Starting from the

* Corresponding author.
E-mail address: ascione@unina.it (A. Ascione).

0040-1951/$ - see front matter © 2006 Elsevier B.V. All rights reserved.
doi:10.1016/j.tecto.2006.04.011

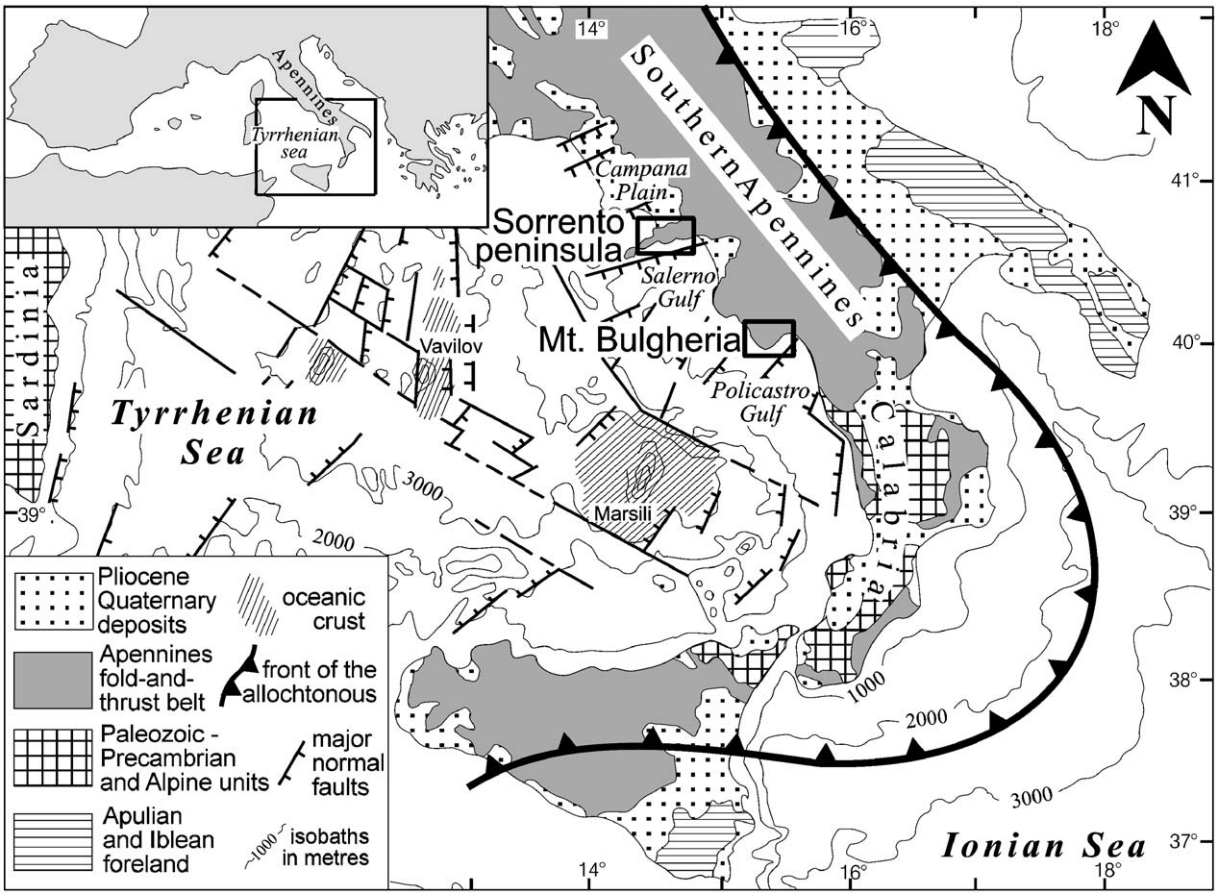

Fig. 1. Structural sketch of the Tyrrhenian basin (modified after Moussat et al., 1986). Frames indicate location of the study areas.

Late Tortonian (Patacca et al., 1990; Sartori, 1990), thrust sheet emplacement proceeded parallel to the extension that led to opening of the Tyrrhenian back-arc basin, and to drowning of the innermost portions of the chain (Malinverno and Ryan, 1986; Patacca et al., 1990; Sartori, 1990).

The Late Tortonian–Middle Pliocene rifting in the Tyrrhenian basin was characterised by an E–W oriented stretching direction, and initiated along the Sardinia margin to migrate eastwards (Sartori, 1990). Post-Middle Pliocene rifting was mostly confined to the southeastern portion of the basin, that was also affected by a strong — not only related to thermal subsidence — Pleistocene subsidence (Sartori, 1990). Since Early Pleistocene, spreading (Savelli and Schreider, 1991) and stretching with a NW–SE orientation (Moussat et al., 1986; Sartori, 1990) are recognised within this portion of the basin.

The Tyrrhenian slope of the belt is characterised by a strong morphostructural fragmentation. This is due to the fact that this side of the chain underwent both shortening and extensional deformation, probably linked to the widening of the adjacent Tyrrhenian Sea: the most striking evidence of the youngest rifting phases is given by wide grabens (Fig. 2), which are partly filled by Pliocene–Quaternary sequences of up to 3 km thick (Ippolito et al., 1973; Bigi et al., 1983; Brancaccio et al., 1991; Brocchini et al., 2001). But in this side of the chain the identification of earlier tectonic events is difficult. This is due to the mentioned complex superposition of compressional and extensional structures with variable orientations and kinematics, and also to the fact that the rare deposits younger than the Late Miocene are mostly continental and often undatable.

In order to unravel the Late Tertiary–Quaternary tectonic history of the Southern Apennines inner slope, we choose two key areas rich in Plio-Quaternary formations and landforms providing useful constraints to the age and amount of the displacements. These areas

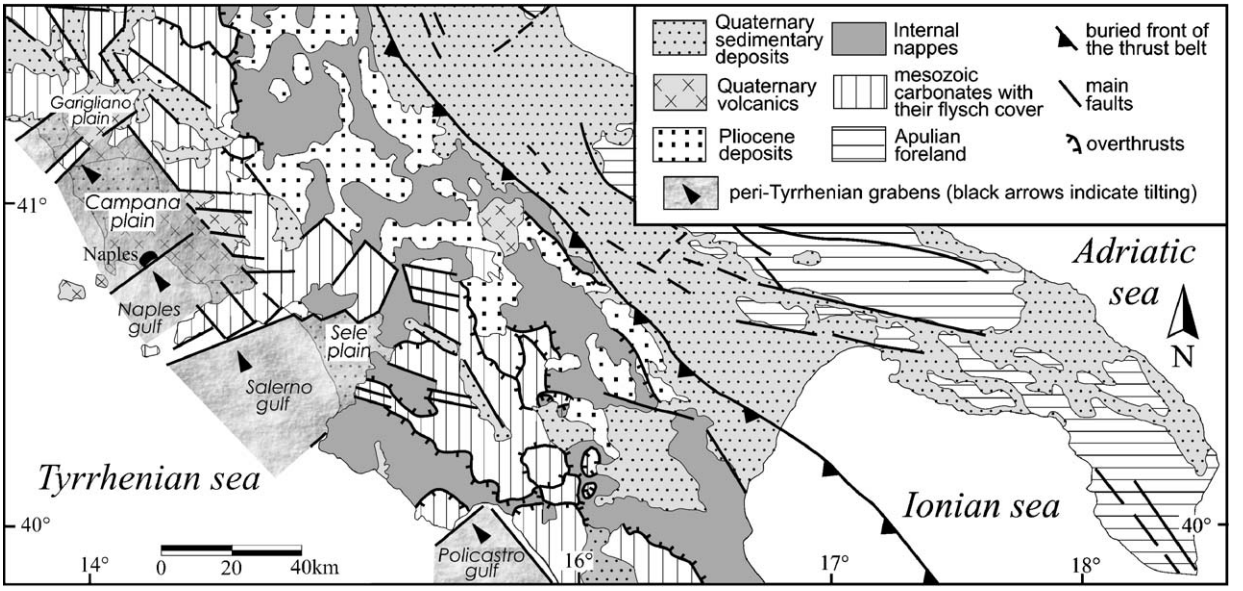

Fig. 2. Simplified geological map of the Southern Apennines (modified after Bigi et al., 1983).

are the two carbonate headlands of the Sorrento peninsula and Mt. Bulgheria.

2. Methods

The approach we used consisted of the combination of structural and morphotectonic analyses.

The structural analysis was addressed by the reconstruction of the stress tensors responsible for the deformation. We used the stress inversion method (Armijo and Cisternas, 1978; Etchecopard et al., 1981; Angelier, 1994) which consists of measuring fault slip movements to derive paleostress tensors. A total amount of 1050 measurements was collected in 32 sites in Mesozoic to Quaternary rocks. The fault slip data were analysed using the stress inversion method of Angelier (1994).

In order to reconstruct the chronology of the tectonic events, we used, besides purely structural criteria (e.g. cross-cut relationships of faults; superposition of striations on fault planes; relationship between the plunge of the stress axes and the bedding attitude, i.e. faulting predating, postdating or inducing the tilting), the cross-cut relationships of structures and deposits and/or erosional landforms of known age. The latter are represented by: fault generated hillslopes (fault scarps, fault line scarps and fault related scarps[1]); shorelines and marine terraces; remnants of sub-planar ancient landscapes of karstic and fluvio-karstic origin, hereafter named paleosurfaces.

The morphotectonic analysis was addressed to obtain further constraints through local reconstructions of sequences of erosional, depositional and faulting events, whose chronology was constrained by the dated deposits. This approach also allowed discriminating older from younger faults by (i) the cross-cut relationships among fault scarps; (ii) the degree of maturity of fault scarps and (iii) the cross-cut relationships between faults and sub-planar landforms, i.e. if the latter are offset (e.g. two terraces/paleosurfaces remnants at different elevation are separated by a straight fault scarp) or seal a fault that was active during one tectonic event. In this case, a terrace/paleosurface remnant cuts across a fault, whose offset may be completely or partly planed off by erosion; in the second case, a fault generated scarp is still present but, due to erosion, it results less straight (in plan view) and retreated with respect to the fault trace.

The morphotectonic study was also devoted to estimation of vertical offsets from: the height of the fault scarps; the amount of displacements affecting indicators of ancient base levels (e.g. strandlines, terraces and slope-toe concavities); the magnitude of fault induced phases of fluvial dissection.

3. Geological setting

Mt. Bulgheria (Fig. 3) is made up of carbonate rocks Upper Triassic to Lower Miocene in age, that are

[1] The term "fault-related scarp" is here referred sensu Ascione et al. (2003) to "*hillslopes whose origin is somehow related to a basal fault plane, but whose height is due to two factors that appear difficult to quantify separately: the active contribution of tectonics and the contribution due to differential erosion*".

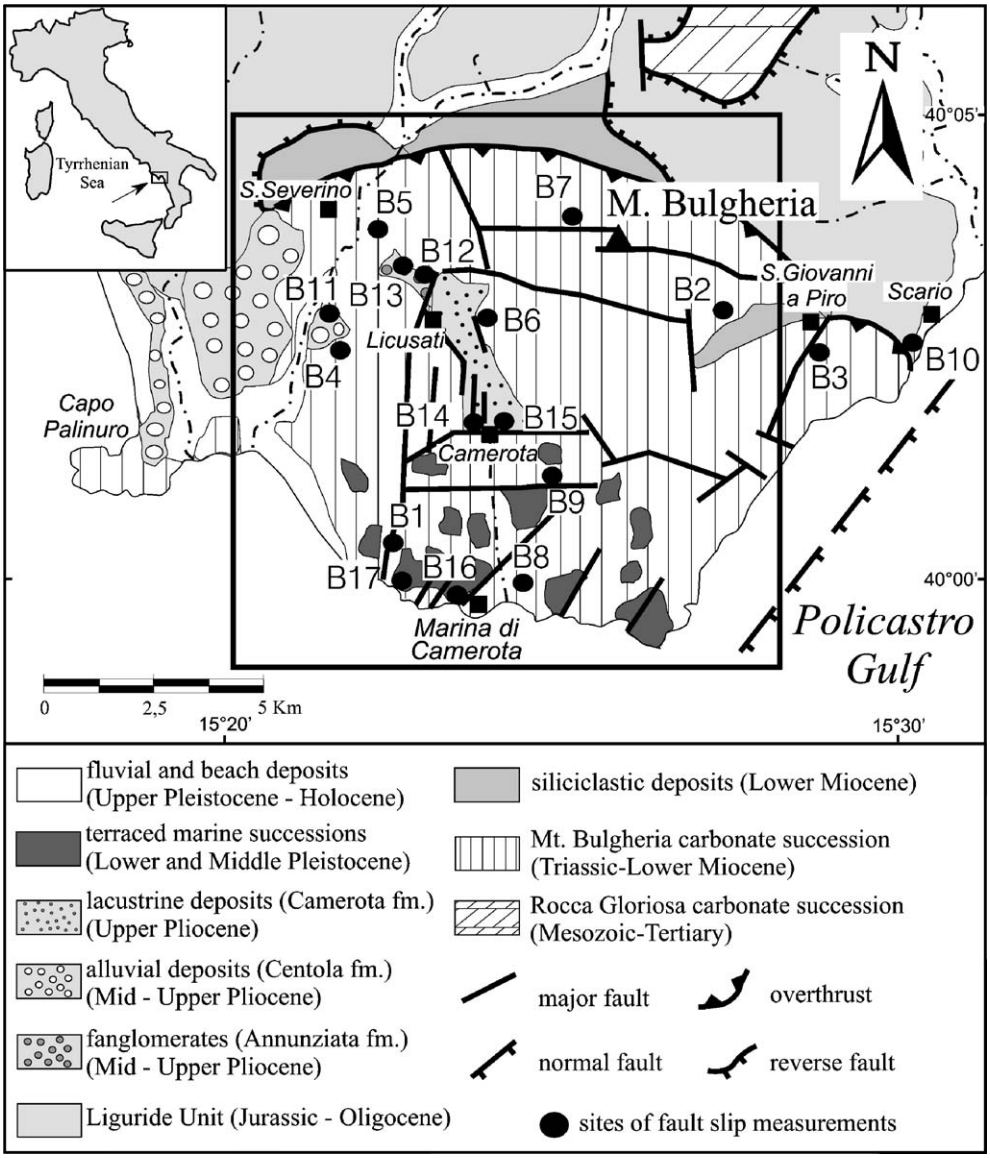

Fig. 3. Simplified geological map of Mt. Bulgheria area. In the frame, the area mapped in Fig. 5.

unconformably covered by Lower Miocene siliciclastic deposits (Scandone et al., 1963). This succession forms a N-verging fold thrusted over the internal Liguride nappe (Tozzi et al., 1996), cut by NE–SW, WNW–ESE, E–W and roughly N–S trending faults. A major NE–SW trending fault borders Mt. Bulgheria towards the Gulf of Policastro peri-Tyrrhenian graben, where the carbonates are lowered to about 3000 m below the sea level (Bigi et al., 1983).

The Sorrento peninsula is part of an ENE–WSW trending ridge that includes also the island of Capri. It is made up of an around 4000 m thick carbonate succession Triassic to Cretaceous in age, covered by Langhian calcarenites that pass into Mid–Upper Miocene siliciclastic deposits (De Blasio et al., 1981) (Fig. 4). The structure of the ridge roughly approximates a NW dipping monocline, thrusted by N-verging carbonate tectonic units (Caiazzo et al., 2000). It is cut by NW–SE trending faults creating a horst-and-graben structure (e.g. Mt. Faito–Mt. Tre Calli horst and the Meta-Sorrento graben; Fig. 4) (Caiazzo et al., 2000). The NW–SE trending faults are truncated by NE–SW trending ones that border the ridge towards both the Salerno Gulf–Sele Plain and the Bay of Naples–Campana Plain peri-Tyrrhenian grabens, where the top of the carbonates are respectively lowered up to 3000 m

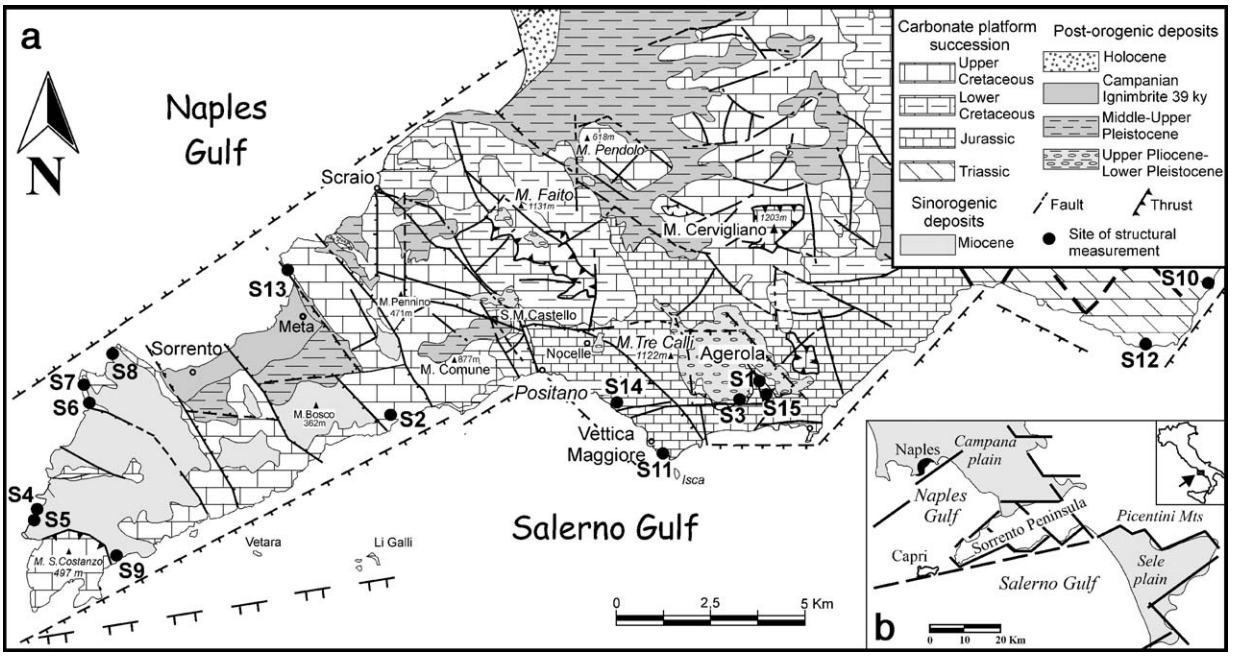

Fig. 4. Geological map of Sorrento peninsula (modified after Caiazzo et al., 2000).

(Moussat et al., 1986) and to 2600 m (Bruno et al., 1998) below the sea level.

In the two study areas, several Plio-Quaternary continental and marine deposits are present. A detailed description of these deposits is given in Chapter 4.

4. Plio-Quaternary deposits and landforms and age constraints

In the two areas, the post-Miocene sedimentary record is scattered and often given by continental undated deposits. The relative ages of these deposits — and of the widespread erosional landforms — were inferred by means of local geomorphological–stratigraphical studies constrained by several chronostratigraphical data.

4.1. Mt. Bulgheria area

In Mt. Bulgheria area, the youngest relic shore deposits and lines, that develop almost continuously along the rocky sea cliffs of the headland, are correlated to Late Pleistocene age last interglacial period (Oxygen Isotope Stage 5; Shackleton and Opdike, 1973). In particular, basing on geochronological data (racemization on Astralium shells, Russo, 1994; Th/U measurements, Esposito et al., 2003), and on comparison of their elevations with global (Lambeck and Chappell, 2001) and local (Mediterranean area; Ulzega and Hearty, 1986) sea-level curves, shorelines ranging from 10 to 6 m a.s.l are correlated to the highest O.I.S. 5 peak (O.I. subStage 5e, about 130 ky old; Shackleton and Opdike, 1973).

Above these shorelines, a flight of uplifted marine terrace develops along the southern coastal belt from around 15 to 130 m a.s.l. (Fig. 5). These terraces consist of abrasion and wave-built (with pebbles and sands, sometimes covered by eolian sands) landforms. They are related to the Middle Pleistocene (a late Lower Pleistocene age might be assigned to the highest and oldest ones) basing on their relationships with the O.I.sS. 5e shorelines and with older deposits. All terraces, in fact, cut across severely offset and, at some places, tilted (up to 20°) marine deposits. These are given by successions made up of silts and clays (that crop out from the sea level up to around 100 m in Cala Bianca area), of beach conglomerates and arenites (cropping out from the sea-level up to around 150 m in the south-western coastal belt), and of conglomerates, arenites, silts and clays that form terraces resting from 200 to around 280 m a.s.l. in Lentiscosa area (Figs. 5 and 6; Ascione et al., 1997). Age of the Cala Bianca and Lentiscosa successions is constrained to the interval ranging from 1.5 to 1.1 Ma basing onto the occurrence of *Hyalinea Baltica* (Ciampo, 1976; Lippmann-Provansal, 1987), that marks the beginning of the Emilian stage of the Early Pleistocene in the Mediterranean area (Pasini and Colalongo, 1994), and of *Hemicytherura*

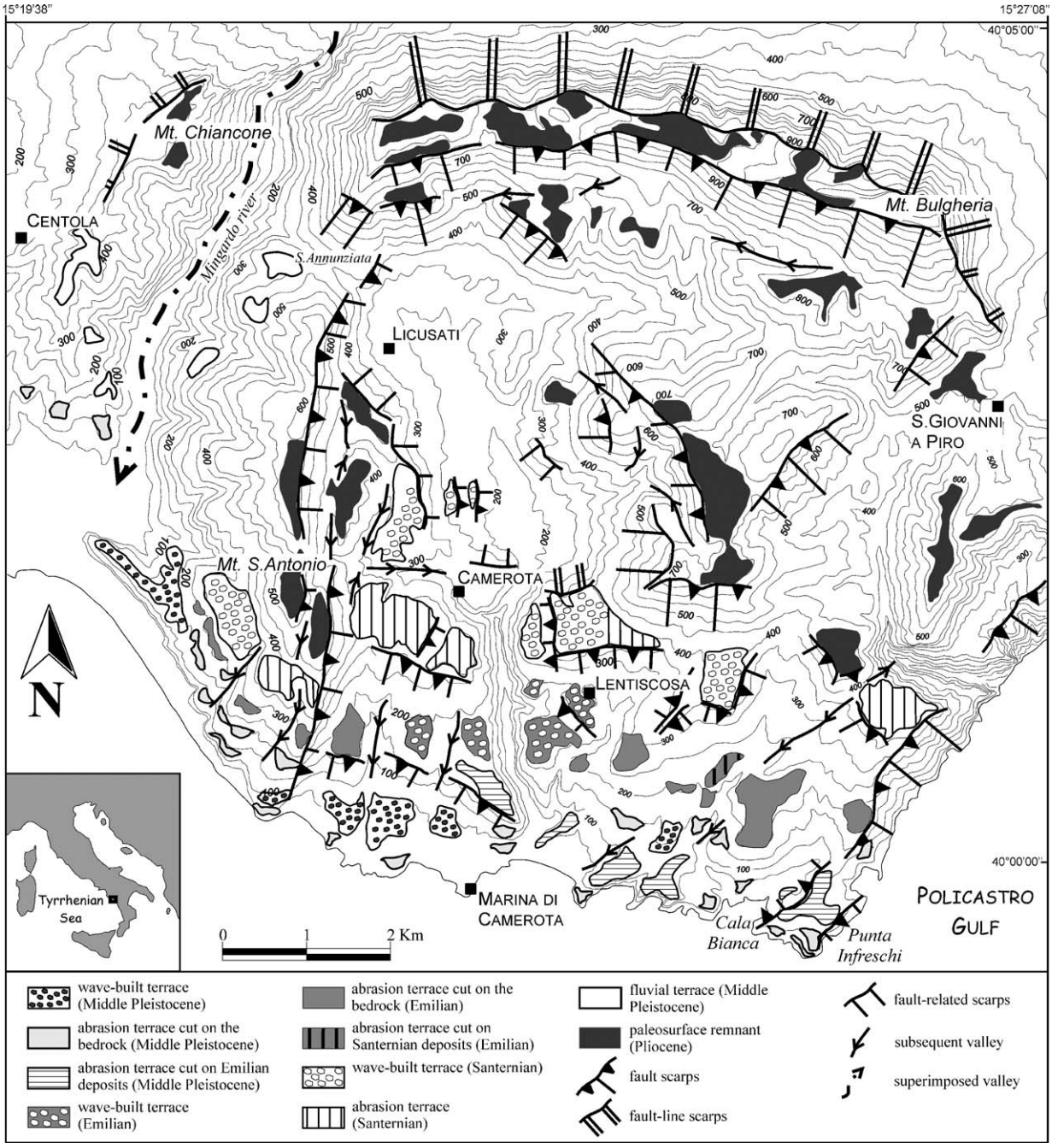

Fig. 5. Morphostructural map of Mt. Bulgheria (modified after Ascione and Romano, 1999). See Fig. 3 for location.

truncata and *Mutulus laticancellatus* (Ciampo, 1976; Borrelli et al., 1988), ostracods restricted to the Emilian (Ciampo, 1976; Bonaduce et al., 1987).

In Lentiscosa area, the Emilian age deposits lay onto the structural sea-cliffs created by faults that had offset older marine terraces: these rest from around 350 to 400 m a.s.l., and mostly consist of abrasion platforms covered by patches of beach pebbles (Ascione and Romano, 1999; Fig. 5). The latter represent the uppermost term of a marine succession (in the lower part made up of sands and silts) that crops out N and around Camerota settlement, from 260 m to around 400 m of elevation (Fig. 6). Age of these deposits is constrained to the interval ranging from 1.84 to

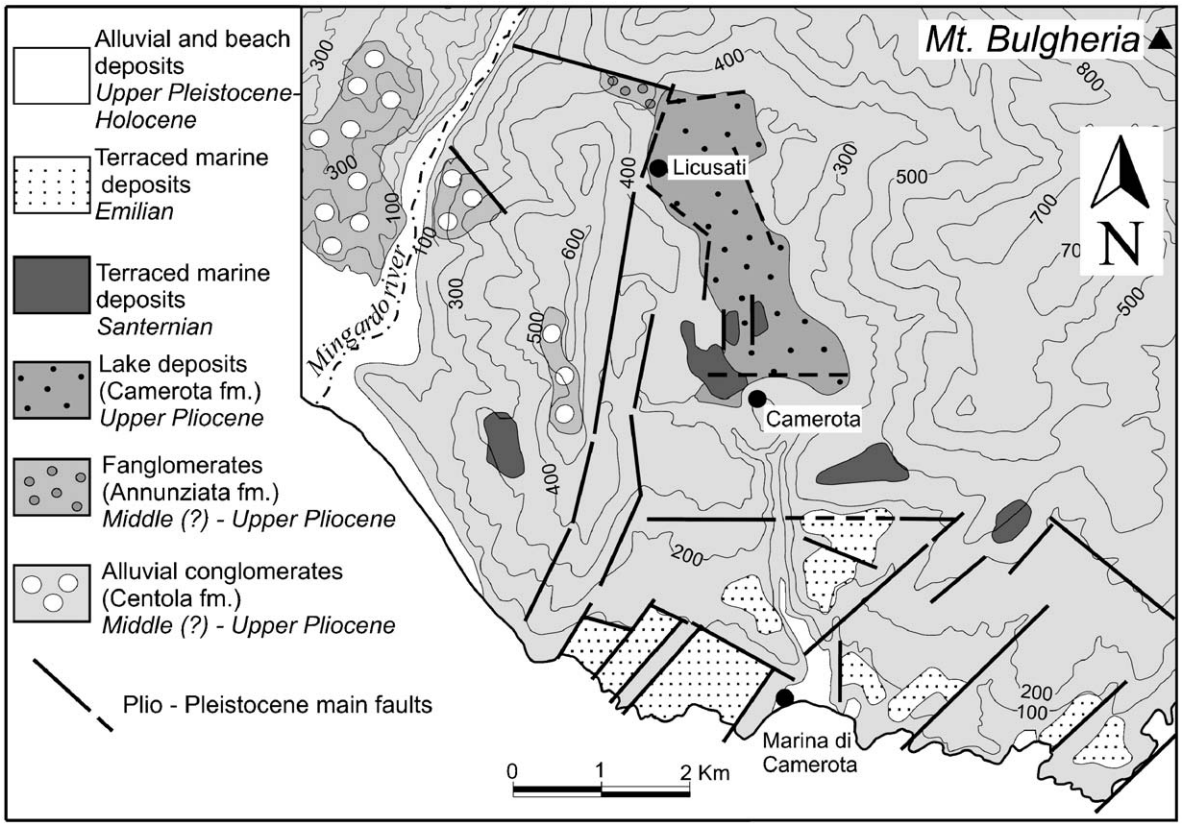

Fig. 6. Map of the Pliocene and Lower Pleistocene deposits cropping out in Mt. Bulgheria area.

1.619 Ma (earliest Pleistocene: Santernian stage), by the occurrence of *Bulimina elegans marginata* (that approximates the Plio-Pleistocene boundary; Pasini and Colalongo, 1994) and of *Calcidiscus macintyrei* (last occurrence of which is dated at 1.619 Ma ago; de Kaenel et al., 1999).

This succession rests on top of lacustrine deposits that occupy a fault bounded basin developed N of Camerota settlement (Camerota basin). By the pollen record of the lake deposits (Lippmann-Provansal, 1987; Russo Ermolli, 1999), it results that elevations up to around 800–1000 m were present around the basin, and that deposition of these sediments postdates onset of the glacial/interglacial cycles, that occurred at 2.6 Ma (Lisiecki and Raymo, 2005). Taking into account age of the overlying marine deposits, the lacustrine deposits (Camerota fm; Fig. 6) result Upper Pliocene in age.

Faults bounding the Camerota basin uplift and offset older continental deposits. One of these is the alluvial (mostly made up of blocks and boulders) Centola fm, that crops out at around 500 m of elevation on top of Mt. S. Antonio and, at various elevations, on the flanks of the Mingardo river valley (Fig. 6). The other one (Annunziata fm) is made up of fanglomerates and crops out at the NW corner of the Camerota basin (Fig. 6). On the basis of their relationships with the Camerota fm, these successions are related to the Mid–Late Pliocene.

An older (Lower-Mid Pliocene) age is assigned to the widespread uplifted, displaced and dissected remnants of paleosurfaces preserved onto the carbonates from around 500 to 1000 m of elevation (Ascione and Romano, 1999; Fig. 5).

4.2. Sorrento peninsula

Along the southern coastal hillslopes of the peninsula, several ancient beach deposits and shorelines (terraces and notches) are present. The ones that develop continuously along the coastal belt between 7.5 and 6.5 m a.s.l., are related to the O.I.sS. 5e (Brancaccio et al., 1978; Cinque and Romano, 1990; Riccio et al., 2001) basing on geochronological data (Th/U measurements; Brancaccio et al., 1978) and/or on their elevation. With the exception of minor height differences among these markers (around 1 m, related to slight vertical offsets; Riccio et al., 2001), their elevation substantially

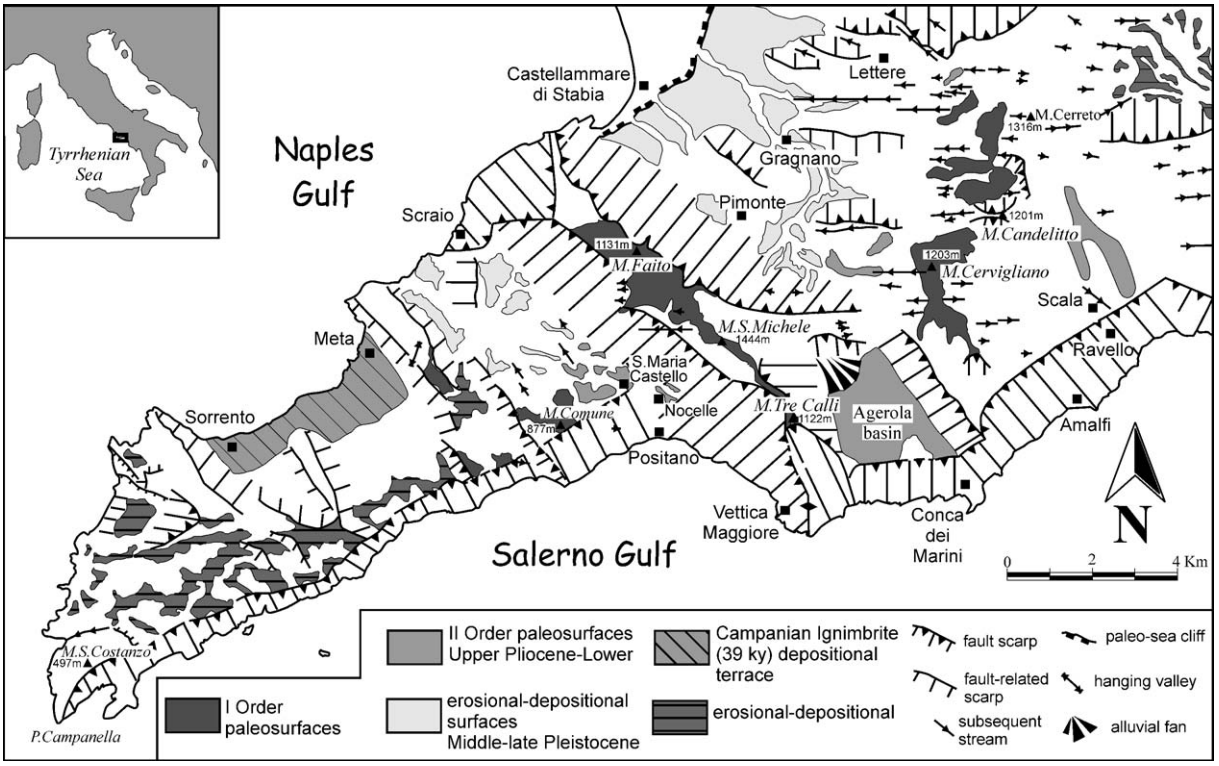

Fig. 7. Morphostructural map of the Sorrento peninsula.

coincides with the one of the O.I.sS. 5e peak in the Mediterranean area.

A higher order of shorelines, at about 8–10 m of elevation, is widespread along the southern sea-cliffs and is related by Cinque and Romano (1990) to the sea-level highstand more closely predating the O.I.S. 5, i.e. the O.I.S. 7, which is around 200 ky old (Lisiecki and Raymo, 2005). Beach deposits and marine terraces tentatively related to the earlier Middle Pleistocene sea-level rise and highstand (O.I.S. 9, which is around 330 ky old; Lisiecki and Raymo, 2005) range in elevation from 50 to only few metres a.s.l. (Cinque and Romano, 1990).

The highest and oldest relic beach deposits, that rest at 200–230 m a.s.l. in Conca dei Marini area (for location, see Fig. 7), are assigned to the initial Middle

Fig. 8. Paleosurfaces and hillslopes related to the NW–SE trending faults transverse to the Sorrento ridge (northern slope of the peninsula, from Sorrento towards the E). In the background, the I Order paleosurface remnant of M. Faito resting on top of the fault scarp related to the NW–SE trending Scraio-Vettica fault; in the foreground, the lowered remnants of the I Order paleosurface (lowered I O.p. in the picture) and a remnant of the younger paleosurface of uncertain age (u.a. paleosurface) resting on top of the fault-line scarp related to the NW–SE trending fault of Meta (see Fig. 7).

Pleistocene (Caiazzo et al., 2000) basing on their much higher elevation relative to the one of the late Middle Pleistocene shorelines. These sediments postdate deposition of older continental sediments, the Nocelle conglomerates (of alluvial fan environment; Amato and Robustelli, 2002) and Agerola slope breccia (Caiazzo et al., 2000), that hang onto the southern coastal hillslopes of the peninsula at elevations of around 700 m and 600 m a.s.l. respectively, and can be related to the Early Pleistocene or Late Pliocene. These N-dipping, untilted, deposits testify to the existence, at the time they were deposited, of elevations to the S, i.e. in the area at present occupied by the Salerno Gulf. These deposits postdate formation of alternating morphostructural highs and lows bordered by NW–SE trending fault scarps: the Agerola breccia occupies the southernmost portion of one of these lows (Agerola basin; Fig. 7), whereas the Nocelle fanglomerates lay onto the SW hillslope of Mt. Faito–Mt. Tre Calli ridge (Fig. 7). These fanglomerates pass laterally to a paleosurface remnant cut on the carbonate bedrock, that is correlated to other ones (hereafter, II Order paleosurfaces; Fig. 7) basing on evidence that they all postdate the NW–SE trending fault scarps. The latter postdate an older paleosurface (I Order paleosurface; Fig. 7), remnants of which are preserved, on top of the highs, up to elevations of 1000–1300 m (Fig. 8). Basing onto the local reconstruction, these landforms may be assigned to the Pliocene.

5. Structural analysis

In the study areas, we measured faults in 32 sites located in rock units of various ages, allowing to derive a chronologically constrained sequence of the paleostress fields. Among the measuring sites (Figs. 3 and 4), 21 were located in carbonate rocks of Triassic to Cretaceous age, in the two areas; 1 site in the Jurassic–Oligocene rocks of the Liguride unit, in Mt. Bulgheria; 3 sites in the Mid–Upper Miocene siliciclastic deposits, in Sorrento peninsula; 5 sites in Mid–Upper Pliocene deposits and 2 sites in Lower Pleistocene littoral conglomerates, in Mt. Bulgheria area. A total of 1050 fault slips was collected from fault planes or striated pebbles. In the paleostress computation, conglomerates with striated pebbles have been treated as similar to pre-fractured rock, with discontinuities in all orientations (Hippolyte, 2001 and references therein).

The senses of fault slip were obtained from observation of steps of calcite, tension tool marks, stylolitic peaks, tensile fractures and Riedel like secondary fractures.

The results of our analysis show that the investigated areas underwent successive deformation events. This is testified by the occurrence of different slip directions on a same fault plane and on fault planes with the same strike and dip, as well as by the observed cross-cut relationships among fault sets, and by the occurrence of different conjugate fault sets linked to different stress fields.

Seven states of stress were recognised: one characterised by a reverse regime, three by extensional and three by strike-slip regimes. Taking into account that different stress regimes characterised by the same directions of the stress axes (i.e. homoaxial) can be interpreted as interrelated by stress permutations, that can occur during a single deformation event (Angelier and Bergerat, 1983), the seven states of stress were finally grouped into four deformation events. This conclusion was also based onto the observation that homoaxial stress regimes were recognised in the same site (e.g. B5, B6, B8, B9, B10, B11, B12, B13, B15, S1, S7, S9 e S13) and/or were characterised by the same relative age in relation to other states of stress.

The first event (D1; Fig. 9 and Table 1), with a NW–SE oriented $\sigma 1$ axis, was characterised by a dominating strike-slip regime responsible for the genesis of conjugate strike-slip faults mainly trending NW–SE and N–S, and subordinately by a reverse regime reconstructed by roughly N–S and E–W oriented faults showing variable kinematics (from reverse to oblique compressional). To the reverse regime are also related outcrop scale folds with NE–SW trending axis. The two homoaxial regimes can be interpreted as interrelated through permutation between the $\sigma 2$ and $\sigma 3$ axes.

Structures related to event D1 were identified in Mesozoic carbonate rocks and in Upper Miocene siliciclastic deposits, while they do not affect the Pliocene–Quaternary ones. In sites S7 and B9, this deformational event appears as responsible for tilting the Mesozoic limestones while, in the same sites, stress fields related to other deformation events postdate the tilting (Fig. 10). As a consequence, this deformation event can be considered as the oldest one.

The second deformation event (D2; Fig. 11 and Table 1) was characterised by two different stress regimes: one strike-slip (roughly N–S oriented $\sigma 1$) and the other extensional (roughly N–S oriented $\sigma 2$) having in common an E–W $\sigma 3$ orientation and interrelated through permutation between the $\sigma 1$ and $\sigma 2$ axes.

Event D2 affected the Mesozoic carbonate rocks (sites S1, S2, S4, S6, S7, S11, S15, S10, B2, B4, B5, B6,

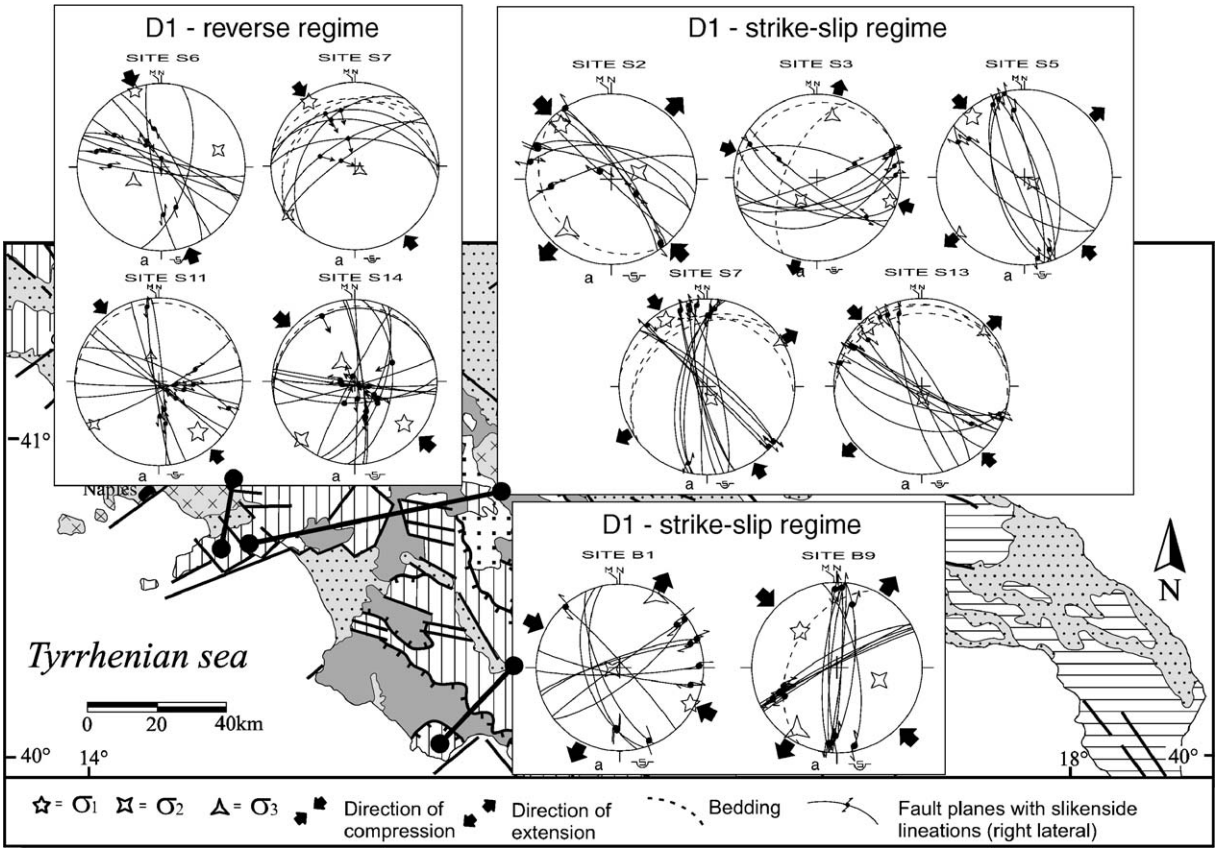

Fig. 9. State of stress related to event D1. States of stress are either strike-slip (σ3 axis oriented NE–SW) or reverse (σ2 axis oriented NE–SW), with a common NW–SE orientation of the σ1 axis.

B8, B9, B12 and B13), the Jurassic–Oligocene Liguride unit (B10), the Mid–Upper Miocene siliciclastic deposits (S5, S8 and S9) and also the Mid–Upper Pliocene formations of Centola (site B11) and Annunziata (sites B12 and B13).

The D2 strike-slip regime created conjugate strike-slip faults, NNE–SSW sinistral and NW–SE to NNW–SSE dextral, and was responsible for reactivation of pre-existing NW–SE trending faults with slightly to strongly oblique strike-slip movements. During the extensional regime, the NW–SE to NNW–SSE trending fault were reactivated with normal to strongly oblique kinematics.

The third deformation event (D3; Fig. 12 and Table 1) was characterised by a NW–SE trending extension direction. Structures related to this event were identified within rock units ranging in age from the Mesozoic to the Lower Pleistocene. In particular, in Mt. Bulgheria area faults related to this event affect the late Upper Pliocene Camerota lacustrine deposits (sites B14 and B15 in Figs. 3 and 13) and Lower Pleistocene conglomerates (sites B16 and B17 in Figs. 3 and 14). Locally (sites S7 and B9), there is evidence that the D3 structures postdate tilting due to the D1 compression (Fig. 10), while at some other places (sites S15, S10, B4 and B5) deformation due to event D3 postdates the tilting of Mesozoic limestones related to event D2 (Fig. 15).

During event D3, extensional and strike-slip regimes with a common orientation of the σ3 axis (NW–SE; Fig. 12) were active in response to permutation between the σ1 and σ2 axes. During the dominant normal regime, newly formed dip-slip NE–SW trending faults were active together with pre-existing NW–SE and N–S trending faults with oblique slip. The D3 strike-slip regime is related to NW–SE sinistral and ENE–WSW dextral transcurrent faults.

The fourth deformation event (D4; Fig. 16 and Table 1) is characterised by extension with σ3 oriented NE–SW. D4 faulting postdates not only tilting due to events D1 and D2 (sites S10, B4 and B5; Fig. 15) but also formation of the D3 structures, as it is inferred from overprinting relations between striations related to events D3 and D4. Conjugate sets of normal faults

Table 1

	Stress state	Faults for tensor calculation	Orientation of paleostress			Φ	ANG	RUP	Latitude	Longitude	Rock type	Age
			σ_1	σ_2	σ_3							
Event D1	Reverse											
	Site S6	10	341 05	074 30	243 60	0.655	18	44	40° 37 06	14° 20 42	Limestones	Upper Cretaceous
	Site S7	6	324 06	234 01	132 84	0.445	15	36	40° 37 05	14° 20 28	Limestones	Upper Cretaceous
	Site S11	10	142 61	237 07	343 22	0.230	23	48	40° 36 32	14° 31 39	Limestones	Jurassic
	Site S14	14	131 22	223 05	326 67	0.633	15	40	40° 37 09	14° 30 47	Limestones	Jurassic
	Strike-slip											
	Site S2	8	317 14	077 63	221 22	0.729	15	47	40° 37 01	14° 26 13	Limestones	Upper Cretaceous
	Site S3	9	108 09	216 63	014 25	0.648	14	43	40° 37 21	14° 33 02	Limestones	Lower Cretaceous
	Site S5	8	319 10	124 80	229 03	0.373	13	42	40° 35 27	14° 19 32	Sandstones	Middle–Upper Miocene
	Site S7	13	328 12	162 78	059 03	0.450	10	42	40° 37 05	14° 20 28	Limestones	Upper Cretaceous
	Site S13	10	318 09	175 78	049 07	0.342	11	42	40° 39 10	14° 24 17	Limestones	Upper Cretaceous
	Site B1	10	117 06	257 82	027 05	0.777	11	28	40° 00 27	15° 21 17	Dolostones	Upper Triassic
	Site B9	12	314 39	107 47	212 14	0.764	11	32	40° 01 26	15° 24 27	Dolomitic limestones	Lower Jurassic
Event D2	Normal											
	Site S1	9	170 69	345 21	076 01	0.209	11	38	40° 37 30	14° 33 26	Limestones	Jurassic
	Site S9	16	063 67	177 10	271 21	0.550	14	33	40° 34 04	14° 21 00	Siliciclastic rocks	Middle–Upper Miocene
	Site S11	6	201 64	006 18	098 05	0.517	26	55	40° 36 32	14° 31 39	Limestones	Jurassic
	Site B6	9	183 58	335 31	076 11	0.493	16	43	40° 03 33	15° 22 41	Limestones	Middle–Upper Miocene
	Site B8	10	167 56	342 28	074 02	0.421	16	46	40° 00 30	15° 22 50	Dolostones	Upper Triassic
	Site B12	12	068 75	182 06	274 13	0.446	17	35	40° 03 44	14° 21 22	Fanglomerates	Middle?–Upper Pliocene
	Site B13	15	193 71	004 19	095 03	0.273	10	30	40° 03 01	15° 21 12	Fanglomerates	Middle?–Upper Pliocene
	Strike-slip											
	Site S1	11	342 05	210 82	073 06	0.455	20	55	40° 37 30	14° 33 26	Limestones	Jurassic
	Site S2	7	197 13	024 77	287 02	0.355	13	32	40° 37 01	14° 26 13	Limestones	Upper Cretaceous
	Site S4	8	174 10	042 75	266 11	0.339	13	40	40° 35 30	14° 19 35	Limestones	Upper Cretaceous
	Site S5	6	006 16	152 71	273 10	0.575	11	25	40° 35 27	14° 19 32	Sandstones	Middle–Upper Miocene
	Site S6	16	355 04	091 60	263 29	0.477	14	38	40° 37 06	14° 20 42	Limestones	Upper Cretaceous
	Site S7	10	004 05	172 85	273 01	0.534	15	36	40° 37 05	14° 20 28	Limestones	Upper Cretaceous
	Site S8	17	175 05	070 74	267 16	0.451	11	34	40° 37 52	14° 20 59	Limestones	Upper Cretaceous
	Site S9	8	013 16	173 73	282 06	0.411	13	32	40° 34 04	14° 21 00	Sandstones	Middle–Upper Miocene
	Site S10	7	342 01	247 77	072 10	0.385	19	40	40° 38 06	14° 41 32	Dolostones	Triassic
	Site S15	5	197 45	030 44	293 07	0.433	10	46	40° 37 12	14° 33 37	Limestones	Jurassic
	Site B2	10	002 15	133 68	268 16	0.759	14	34	40° 02 18	15° 24 56	limestones and marls	Lower Jurassic
	Site B4	11	331 17	129 72	239 07	0.601	13	38	40° 03 16	15° 19 06	Limestones and marls	Lower Jurassic
	Site B5	22	160 09	043 71	252 16	0.736	19	41	40° 04 36	15° 19 38	Limestones	Upper Jurassic–Lower Cretaceous
	Site B6	19	338 16	169 74	069 03	0.513	14	44	40° 03 33	15° 22 41	Limestones	Middle–Upper Jurassic
	Site B7	7	357 22	166 68	265 04	0.625	07	28	40° 05 03	15° 22 37	Limestones	Middle–Upper Jurassic
	Site B9	20	169 08	336 82	079 02	0.408	11	25	40° 01 27	15° 24 47	Dolomitic limestones	Lower Jurassic
	Site B10	11	344 22	172 68	075 03	0.441	15	39	40° 02 38	15° 29 11	Shales (Liguride unit)	Jurassic–Oligocene
	Site B12	19	165 03	320 77	074 05	0.550	10	24	40° 03 44	15° 21 22	Fanglomerates	Middle?–Upper Pliocene

(continued on next page)

Table 1 (*continued*)

	Stress state	Faults for tensor calculation	Orientation of paleostress			Φ	ANG	RUP	Latitude	Longitude	Rock type	Age
			σ_1	σ_2	σ_3							
Event D2	Site B13	15	195 41	013 49	104 01	0.518	12	29	40° 03 01	15° 21 12	Fanglomerates	Middle?–Upper Pliocene
Event D3	Normal											
	Site S1	9	068 69	260 21	169 04	0.558	15	35	40° 37 30	14° 33 26	Limestones	Jurassic
	Site S6	5	316 63	076 14	171 16	0.285	18	52	40° 37 06	14° 20 42	Limestones	Upper Cretaceous
	Site S7	13	276 68	033 11	127 20	0.249	17	44	40° 37 05	14° 20 28	Limestones	Upper Cretaceous
	Site S11	12	053 61	260 22	164 09	0.314	18	42	40° 36 32	14° 31 39	Limestones	Jurassic
	Site S12	7	029 70	236 18	144 08	0.453	08	30	40° 38 12	14° 40 29	Dolostones	Triassic
	Site S13	9	298 74	044 05	135 15	0.270	10	43	40° 39 10	14° 24 17	Limestones	Upper Cretaceous
	Site S14	12	231 71	052 19	322 00	0.418	14	35	40° 37 09	14° 30 47	Limestones	Jurassic
	Site S15	13	200 77	068 09	337 10	0.325	10	25	40° 37 12	14° 33 37	Limestones	Jurassic
	Site B2	13	350 84	222 04	131 05	0.497	15	47	40° 02 18	15° 24 56	Limestones and marls	Lower Jurassic
	Site B4	6	356 76	246 05	155 13	0.577	18	53	40° 03 16	15° 19 56	Limestones and marls	Lower Jurassic
	Site B5	12	240 57	060 33	150 00	0.345	16	38	40° 04 36	15° 19 38	Limestones	Upper Jurassic–Lower Cretaceous
	Site B8	7	145 60	053 26	239 02	0.357	17	40	40° 00 30	15° 22 50	Dolostones	Upper Triassic
	Site B9	7	324 75	060 02	151 15	0.643	07	30	40° 01 27	15° 24 47	Dolomitic limestones	Lower Jurassic
	Site B10	14	009 85	242 03	152 04	0.225	14	46	40° 02 38	15° 29 11	Shales (Liguride unit)	Jurassic–Oligocene
	Site B11	9	247 65	064 25	154 01	0.365	16	36	40° 03 22	15° 19 44	Alluvial conglomerates	Middle?–Upper Pliocene
	Site B14	12	123 79	225 02	315 10	0.492	07	29	40° 01 57	15° 22 02	Lacustrine silts	Upper Pliocene
	Site B15	6	228 75	044 15	135 01	0.523	07	18	40° 01 50	15° 22 08	Lacustrine silts	Upper Pliocene
	Site B16	9	212 77	043 13	313 03	0.507	06	27	40° 00 00	15° 21 49	Marine conglomerates	Lower–Middle Pleistocene
	Site B17	8	247 51	032 34	135 18	0.545	05	20	39° 59 56	15° 21 35	Marine conglomerates	Lower–Middle Pleistocene
	Strike-slip											
	Site S5	8	254 10	052 80	163 04	0.609	11	29	40° 35 27	14° 19 32	Sandstones	Middle–Upper Miocene
	Site S7	14	221 15	085 70	314 14	0.506	13	43	40° 37 05	14° 20 28	Limestones	Upper Cretaceous
	Site S8	10	248 25	084 59	342 06	0.669	12	34	40° 37 52	14° 20 59	Limestones	Upper Cretaceous
	Site S10	5	253 04	102 83	343 02	0.413	20	47	40° 38 06	14° 41 32	Limestones	Triassic
	Site S13	9	237 00	147 84	328 06	0.306	17	36	40° 39 10	14° 24 17	Limestones	Upper Cretaceous
	Site B3	14	068 04	166 63	336 27	0.248	08	26	40° 03 03	15° 26 53	Limestones	Middle–Upper Jurassic
	Site B7	7	080 21	299 64	176 15	0.529	09	33	40° 05 03	15° 22 37	Limestones	Middle–Upper Jurassic
	Site B8	13	044 03	142 65	312 20	0.489	14	52	40° 00 30	15° 22 50	Dolostones	Upper Triassic
	Site B9	10	237 04	114 83	327 06	0.511	12	37	40° 01 27	15° 24 47	Dolomitic limestones	Lower Jurassic
	Site B10	15	059 03	314 78	150 12	0.508	14	40	40° 02 38	15° 29 11	Shales (Liguride Unit)	Jurassic–Oligocene
	Site B11	6	263 19	074 71	172 03	0.325	12	42	40° 03 22	15° 19 44	Alluvial conglomerates	Middle?–Upper Pliocene
	Site B15	10	057 26	245 64	149 03	0.647	10	30	40° 01 50	15° 22 08	Lacustrine silts	Upper Pliocene
Event D4	Normal											
	Site S1	12	122 80	283 09	013 03	0.365	14	45	40° 37 30	14° 33 26	Limestones	Jurassic
	Site S2	5	118 52	331 33	230 16	0.599	13	52	40° 37 01	14° 26 13	Limestones	Upper Cretaceous
	Site S4	6	129 74	283 12	014 06	0.455	20	55	40° 35 30	14° 19 35	Limestones	Upper Cretaceous
	Site S6	19	050 73	152 03	243 17	0.322	09	27	40° 37 06	14° 20 42	Limestones	Upper Cretaceous
	Site S8	6	096 71	323 13	230 13	0.694	19	45	40° 37 52	14° 20 59	Limestones	Upper Cretaceous
	Site S10	5	126 58	297 27	029 03	0.435	09	36	40° 38 06	14° 41 32	Limestones	Triassic
	Site S14	8	106 68	326 17	231 13	0.309	07	27	40° 37 09	14° 30 47	Limestones	Jurassic

Table 1 (*continued*)

	Stress state	Faults for tensor calculation	Orientation of paleostress			Φ	ANG	RUP	Latitude	Longitude	Rock type	Age
			σ_1	σ_2	σ_3							
Event D4	Site B2	4	163 83	301 05	032 05	0.706	04	22	40° 02 18	15° 24 56	Limestones and marls	Lower Jurassic
	Site B4	7	253 80	148 03	058 10	0.364	09	24	40° 03 16	15° 19 56	Limestones and marls	Lower Jurassic
	Site B5	7	259 80	135 05	044 08	0.597	09	26	40° 04 36	15° 19 38	Limestones	Upper Jurassic–Lower Cretaceous
	Site B12	7	162 70	324 19	056 06	0.586	12	43	40° 03 44	15° 21 22	Fanglomerates	Middle?–Upper Pliocene

with NW–SE trend (sites S1, S2, S10 and B4) were created by this event, that caused also widespread re-activations of pre-existing fault planes with an overall oblique slip (sites S4, S6, S8, S14, B2, B5, and B12 in Fig. 16).

6. Reconstruction of tectonic events

In this chapter we reconstruct the chronology of the recognised tectonic events by combining the structural and morphotectonic data from the two study areas. To do that, we discuss in detail the main effects of each deformation event, starting from the oldest.

6.1. Event D1

This event is characterised by a $\sigma 1$ axis trending NW–SE in a dominating strike-slip regime and subordinately reverse regime.

To event D1, that basing on structural data is the oldest one, we relate the major NW–SE right-lateral strike-slip faults affecting the Mesozoic to Miocene rocks cropping out in the Sorrento area. These faults were responsible for the initial fragmentation of the present peninsula: here they outlined a structural setting favourable to the preservation, within structural lows, of the soft siliciclastic units covering the hard carbonate rocks, and to their dismantling in intervening highs.

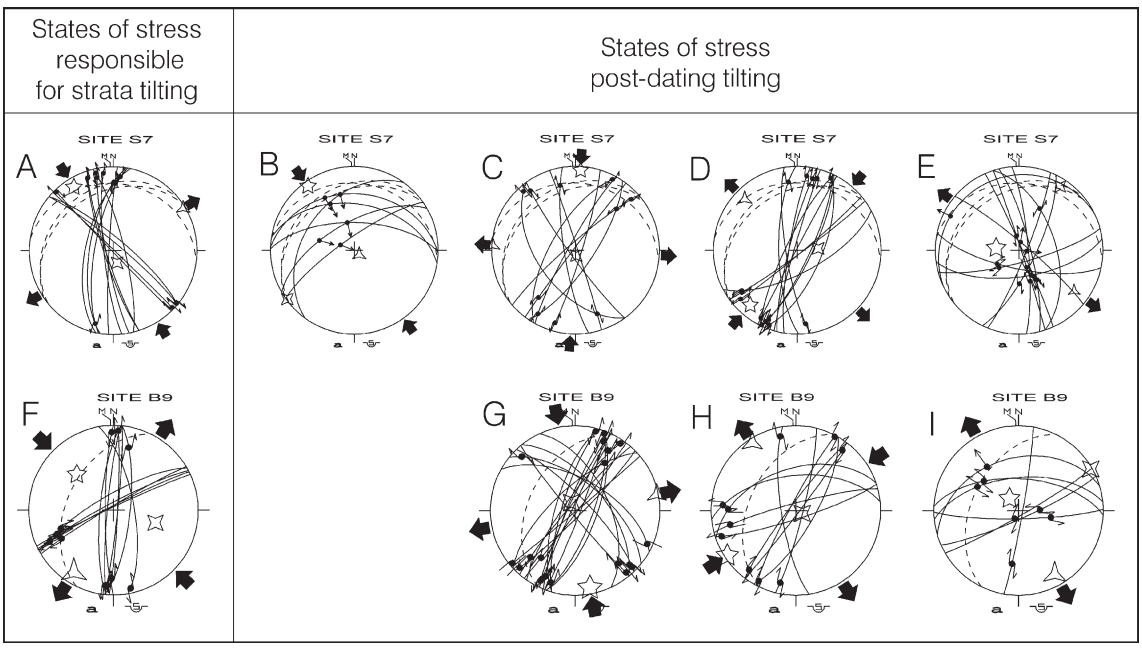

Fig. 10. State of stress obtained from fault slip data in sites S7 and B9. Plots A, B and F are related to event D1; plots C and G to event D2; plots D, E, H and I to event D3. States of stress A and F are responsible for bedding plane tilt (axes $\sigma 1$ and $\sigma 3$ are parallel to stratification and $\sigma 2$ axis is perpendicular to the tilted strata), whereas the remaining post-date tilting (two stress axes are horizontal and one is vertical).

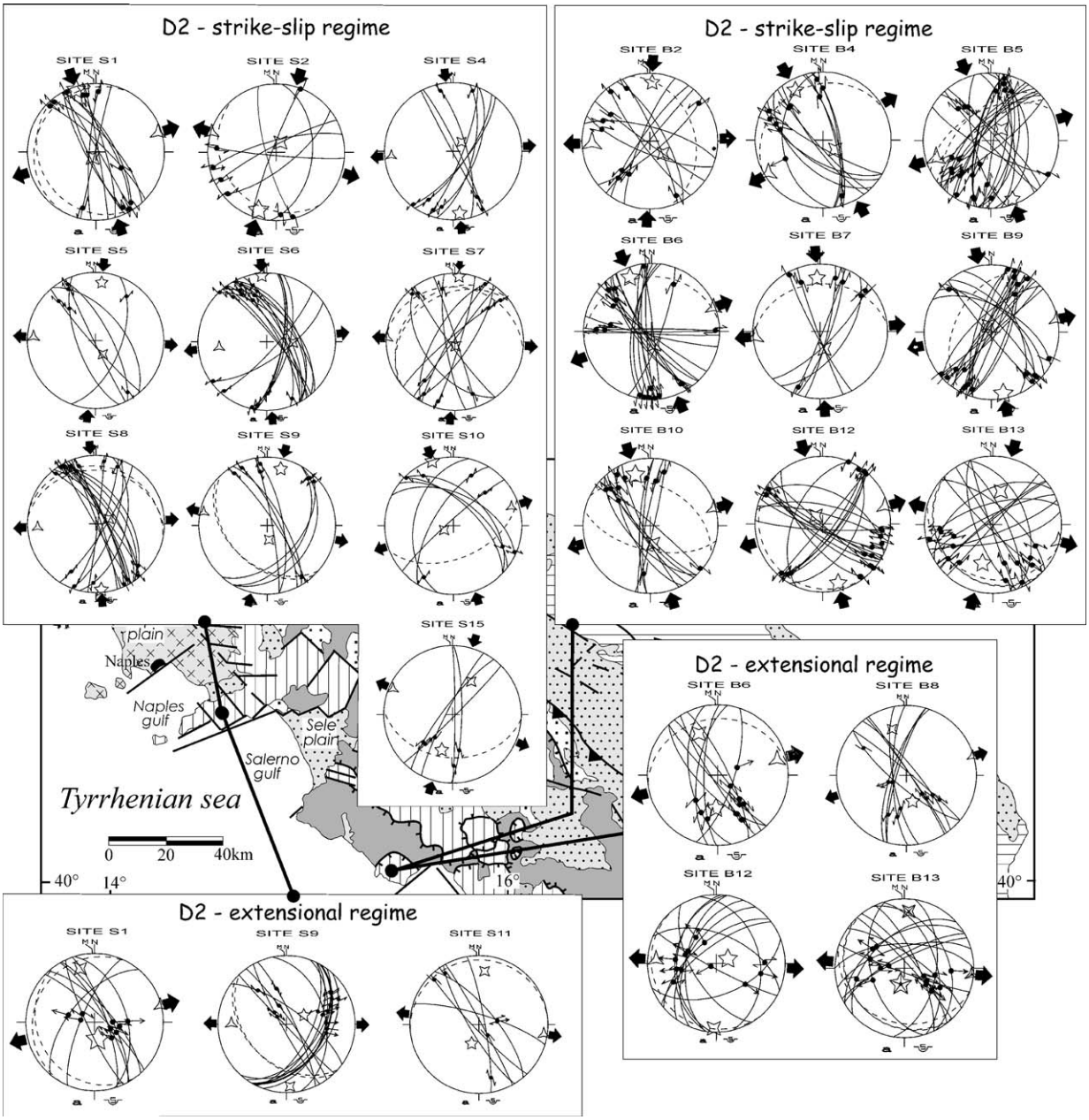

Fig. 11. State of stress related to event D2. It is characterised by a strike-slip regime (σ1 axis roughly oriented N–S) and by an extensional regime, with a common E–W orientation of the σ3 axis. Keys as in Fig. 9.

To this event we also relate fold-related tilting of Mesozoic rocks and minor E–W trending faults in the two study areas. In Mt. Bulgheria area, the structural features that formed during event D1 have little morphological evidence, not only because much smoothed by erosion, but also because overprinted by re-activations and/or strongly displaced by subsequent deformation events.

Event D1 presumably initiated during Mid–Late Miocene times, after the paraconformable deposition of the Langhian calcarenites onto the Cretaceous limestones of the Sorrento peninsula.

6.2. Event D2

The deformational event D2 was characterised by a strike-slip regime (roughly N–S oriented σ1 and E–W trending σ3) and by a homoaxial extensional regime.

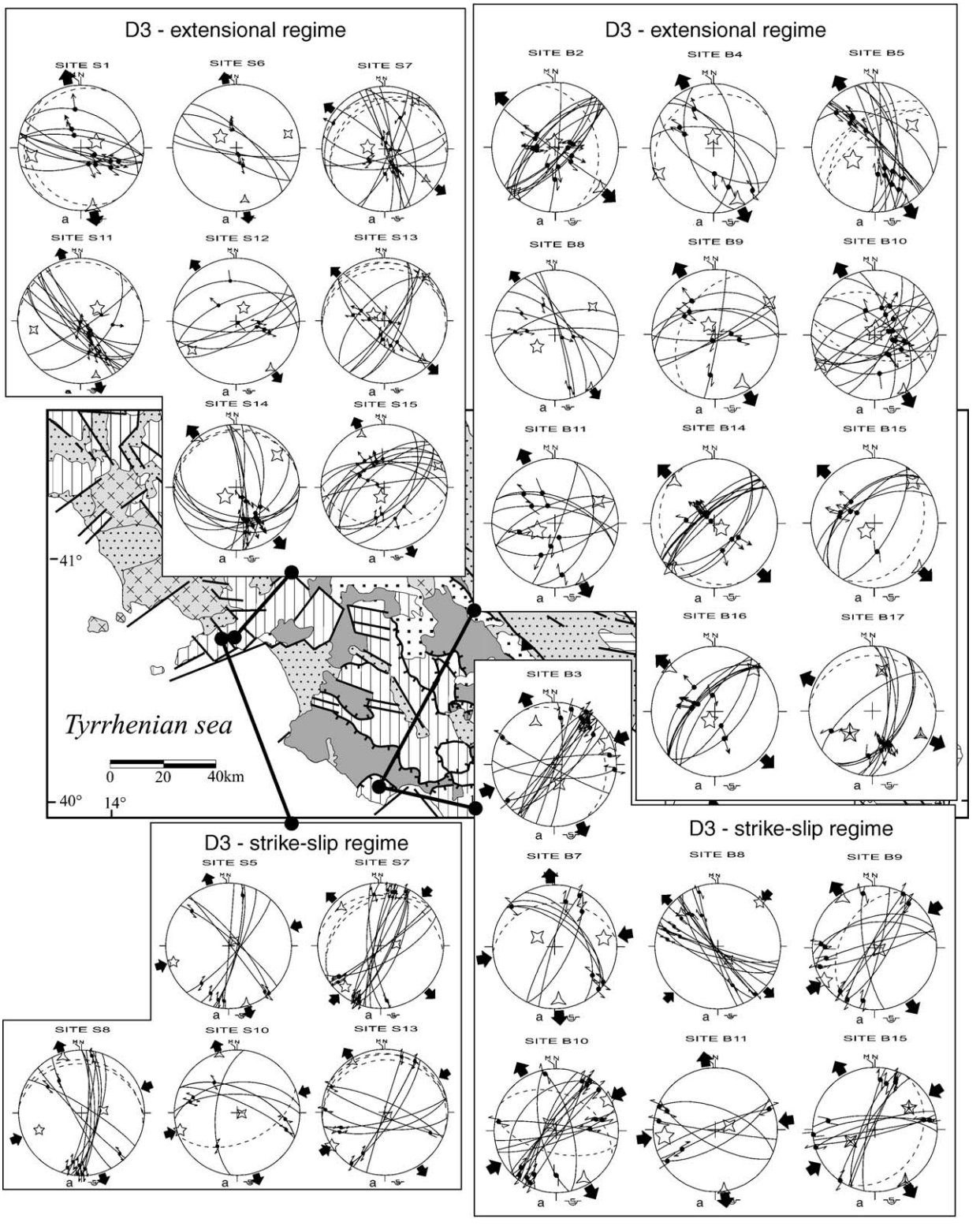

Fig. 12. State of stress related to event D3. It is characterised by an extensional and by a strike-slip (σ1 oriented NE–SW) regime with a common NW–SE oriented σ3 axis. Keys as in Fig. 9.

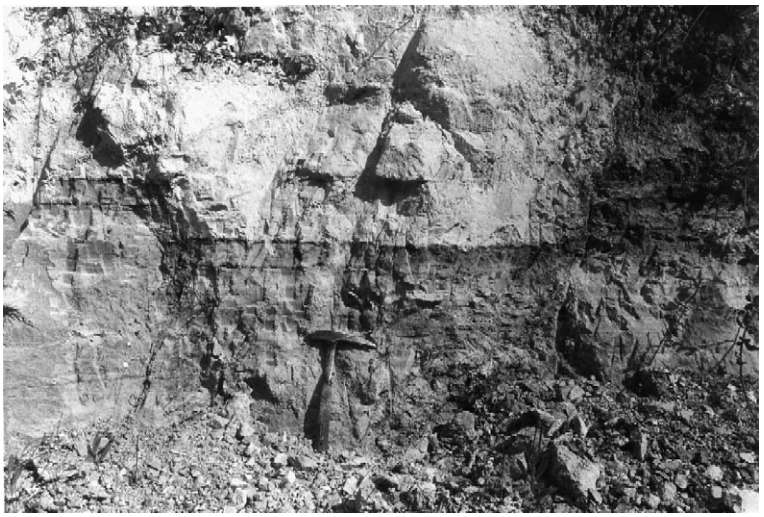

Fig. 13. NE–SW trending conjugate normal faults affecting the Upper Pliocene lacustrine deposits cropping out in Camerota town (Site B14 in Fig. 3).

To the strike-slip regime we relate the N-verging anticline (with E–W axis) of Mt. Bulgheria. In the Sorrento peninsula, it was responsible for the creation and re-activation of major right-lateral, locally transpressive, faults with NW–SE trend, along which some palm-tree structures were generated (Caiazzo et al., 2000). This faulting was coeval to the N-verging overthrusts of Mt. S. Costanzo, Agerola, Mt. Cervigliano and Mt. Faito (Fig. 4), that were emplaced over a bedrock that had already been offset by NW–SE trending faults related to event D1. Since emplacement of these overthrusts took place after most of the Mid–Upper Miocene siliciclastic cover had been eroded in the highest fault-bounded blocks created by the D1, initiation of event D2 can be placed from the final part of the Miocene to the earliest Pliocene.

In the two study areas, the compressional and transpressive structures created by the D2 strike-slip regime predate the highest and oldest paleosufaces. The latter were subsequently displaced by N–S to NW–SE trending faults with large vertical offsets creating horst-and-graben structures (Figs. 17a and 18a). These structures can be related to the D2 extensional regime that, basing on the structural data, was responsible for

Fig. 14. NE–SW trending normal fault; in the footwall crop out Mesozoic limestones and in the hangingwall the Emilian age marine deposits (Site B16 in Fig. 3).

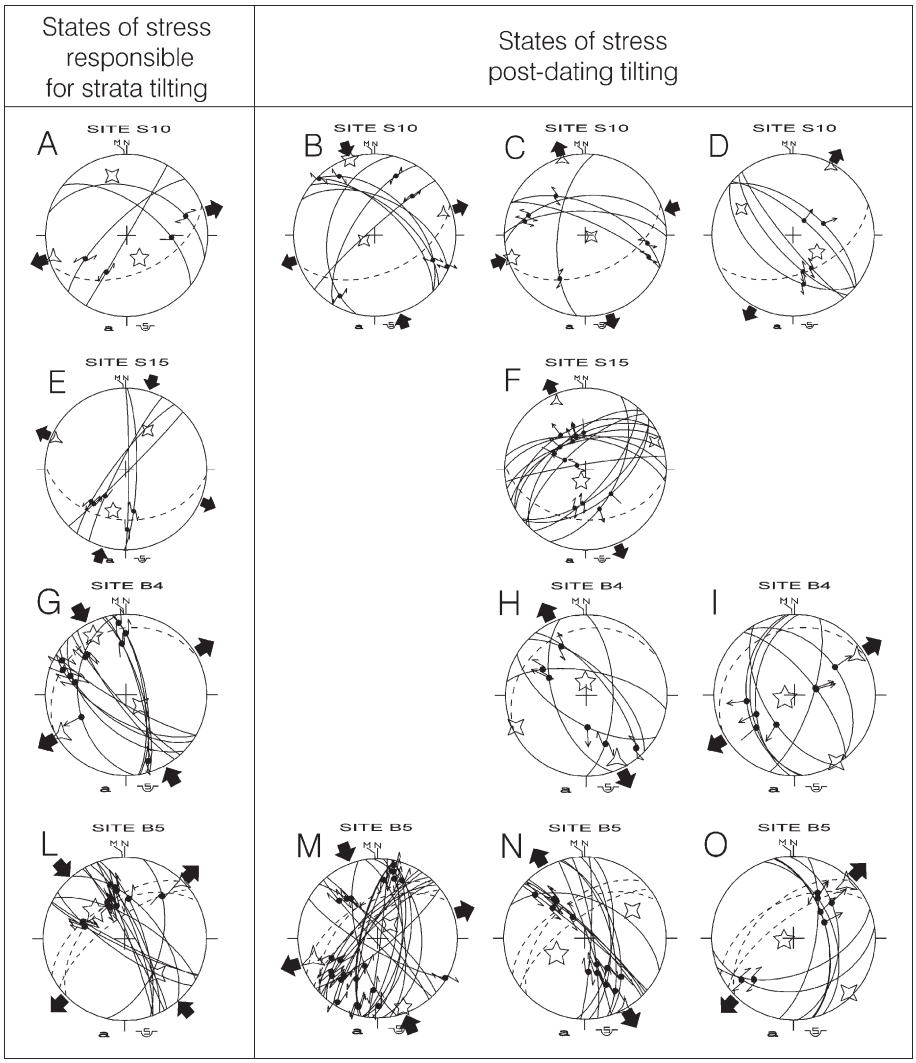

Fig. 15. States of stress obtained from fault slip data in sites S10, S15, B4 and B5. Plots A, B, E, G, L and M are related to event D2; plots C, F, H and N to event D3; plots D, I and O to event D4. Stress A, E, G and L are responsible for strata tilting (axes $\sigma 1$ and $\sigma 3$ are parallel to stratification while, the $\sigma 2$ axis is perpendicular to the tilted strata), whereas the remaining states of stress post-date tilting (two axes are horizontal and one is vertical).

re-activation of NW–SE to NNW–SSE trending faults with normal or strongly oblique strike-slip kinematics.

By this reconstruction, it results that event D2 was dominated in the first period by the strike-slip regime, whereas the extensional regime dominated during the second time period. The D2 extension is well constrained by formation of the Late Pliocene Camerota lake basin in Mt. Bulgheria area. In fact, to the D2 extensional faulting (that affected also the Mid–Upper Pliocene deposits of the Annunziata and Centola fms) are related offsets on the order of some hundreds of metres along NW–SE and N–S trending faults that created the Camerota lake basin (Fig. 17b). This extension also caused local reactivations of segments of some older E–W trending faults as transfer faults: this is demonstrated by the presence, at the southern border of the basin, of older paleosurfaces remnants (at present resting around 500–700 m a.s.l.; Fig. 5) sealing the lateral prosecution of the activated segments of the E–W faults.

In the Sorrento ridge, the D2 extensional faulting caused a strong vertical fragmentation of the I Order paleosurface (e.g. offset up to 600 m along the Scraio-Vettica Maggiore fault zone) and led to the development, along NW–SE to N–S faults, of a horst-and-graben structure which includes also the Agerola basin (Fig. 18a). Slope and alluvial sediments were then deposited in the Agerola basin and in Nocelle area,

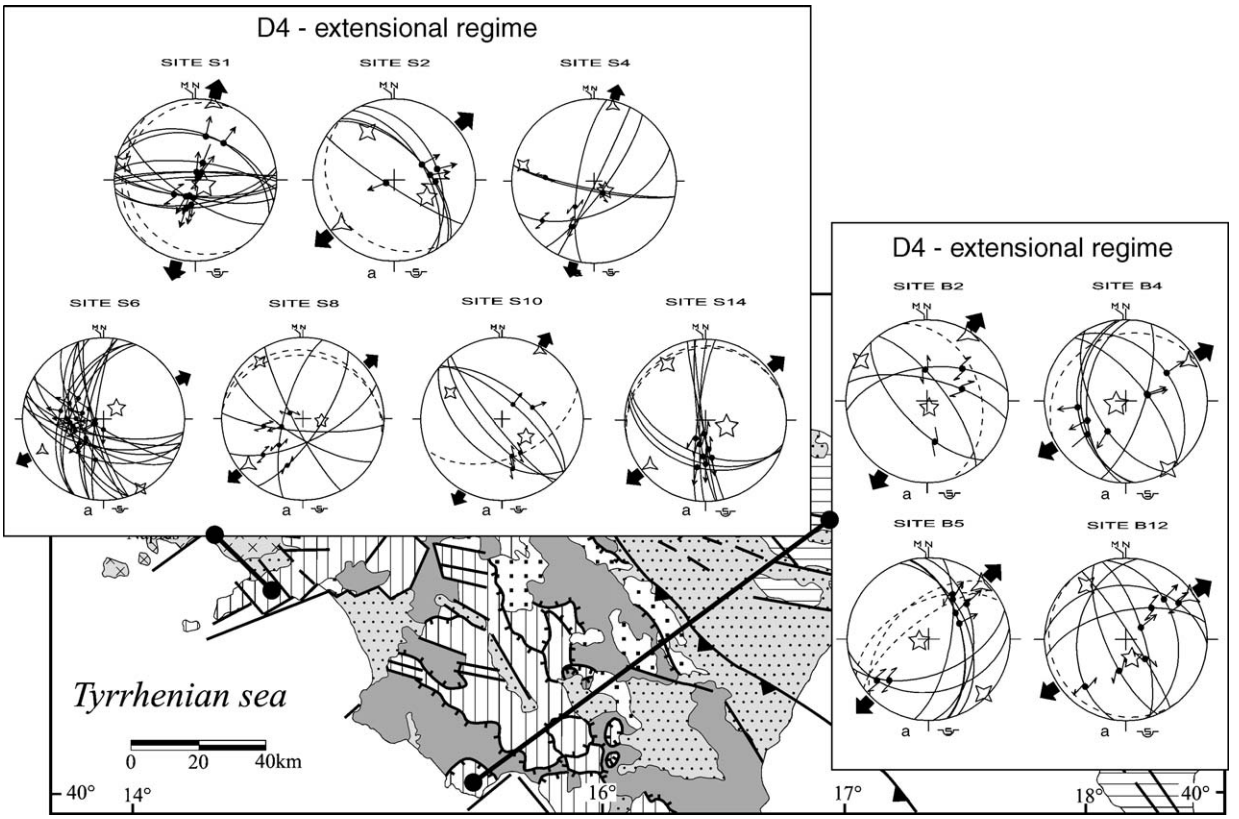

Fig. 16. Stress diagrams related to event D4. They are characterised by an extensional regime with a NE–SW oriented $\sigma 3$ axis. Keys as in Fig. 9.

whereas elsewhere karst processes formed new erosional surfaces (II Order paleosurfaces; Fig. 7) on top of the downfaulted blocks (Fig. 18b).

6.3. Event D3

This event was characterised by NW–SE trending extension direction responsible for a dominant extensional regime, that created major NE–SW trending normal faults with offsets ranging from some hundreds to some thousands of metres. Subordinately, at the outcrop scale, a strike-slip regime is also recorded.

To this event, that initiated not earlier than the Late Pliocene (when the Camerota basin was formed in response to D2), we relate the succession of faulting episodes recorded in the study areas during most of the Pleistocene.

In Mt. Bulgheria, the sequence of Early Pleistocene faulting episodes is well constrained by the Lower Pleistocene marine deposits and landforms. In particular, the Santernian marine deposits and terraces (Fig. 17c) record a first faulting episode by mainly NE–SW and some E–W and NW–SE trending faults with offsets on the order of some hundreds of metres (Fig. 17d); minor (10–20 m) offsets by few N–S trending faults are also recorded. Subsequently, during the Emilian, the area was partly submerged with deposition of marine sediments that seal faults created during the post-Santernian event (Fig. 17e). A further faulting episode displaced the Emilian age terraces (Fig. 17f) with offsets on the order of hundreds of metres. It was related to some NW–SE trending faults, and to major and widespread NE–SW trending faults that created a horst-and-graben structure in the southernmost portion of the area (Fig. 14), and also the tectonic sea-cliff that at present bounds Mt. Bulgheria towards the Policastro Gulf. The lateral continuity of the Middle Pleistocene terraces and shorelines indicates the substantial ceasing of this widespread faulting, and suggests that since the Middle Pleistocene activity was mostly confined to the NE–SW trending fault bounding the headland towards the Policastro Gulf, where the carbonates are lowered to about 3000 m below the sea level.

The combined structural and morphotectonic evidence from Mt. Bulgheria shows that the NE–SW trending are neo-generated normal faults; the E–W trending ones (that consist of re-activated portions of older and longer structures, partly sealed by the Pliocene

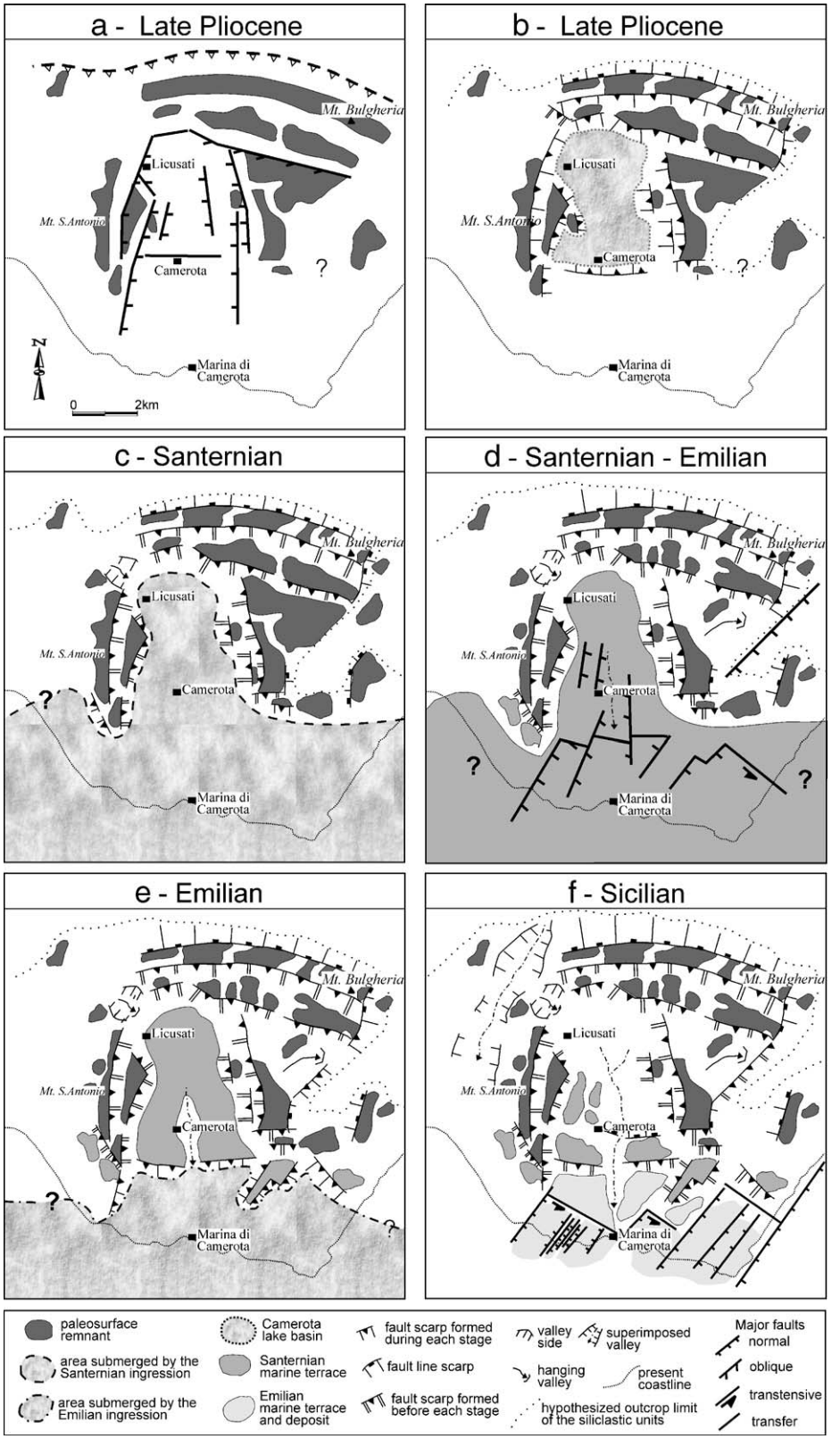

Fig. 17. Palaeogeography of Mt. Bulgheria area from the Late Pliocene to the late Early Pleistocene. (Modified after Ascione and Romano, 1999).

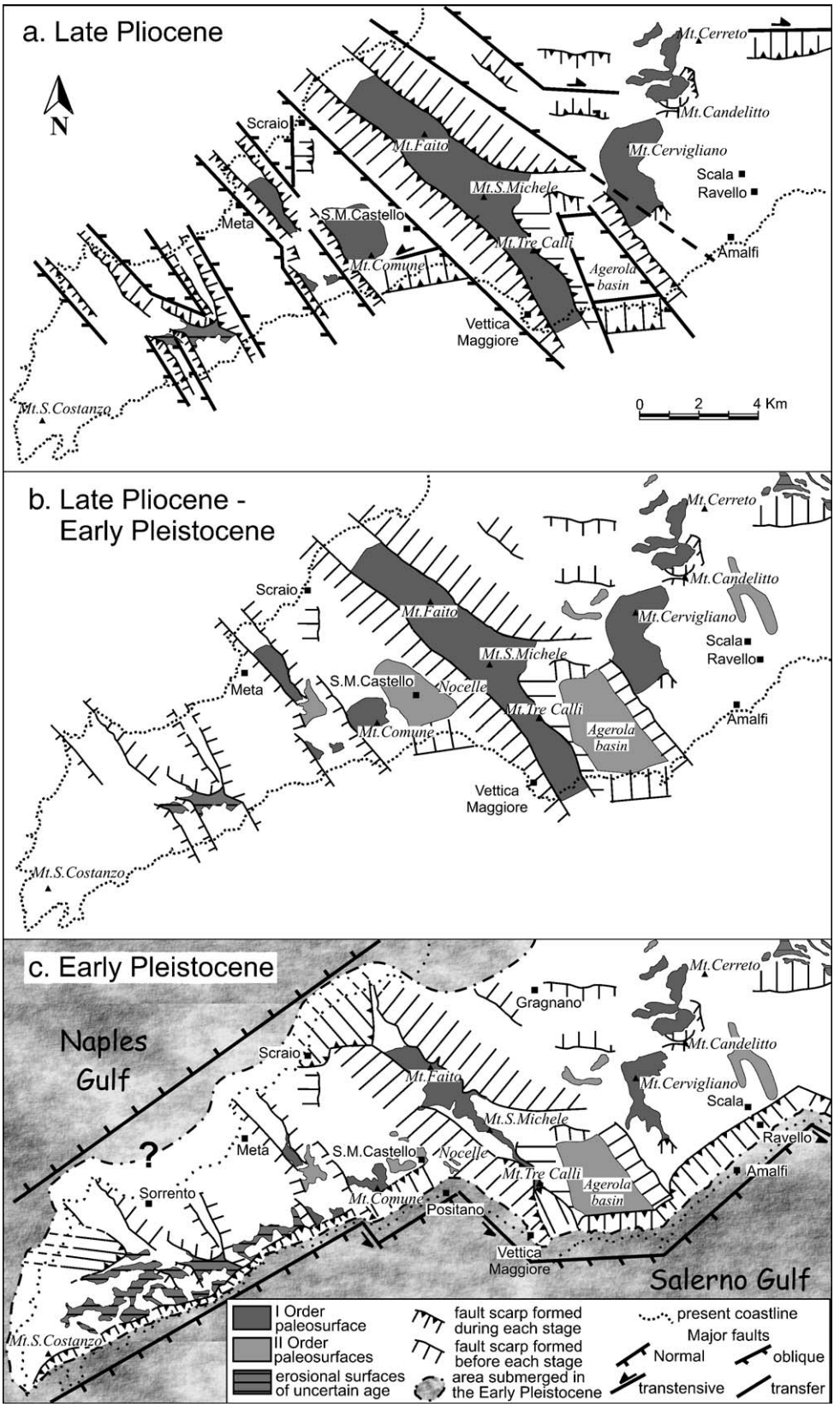

Fig. 18. Palaeogeography of the Sorrento peninsula during Late Pliocene and Early Quaternary.

paleosurfaces at 500–700 m) can be interpreted as transfer faults, whereas the NW–SE and the rare N–S trending as strike-slip and oblique transtensive faults respectively.

During event D3, in the Sorrento area, major NE–SW trending normal faults were created; some NW–SE trending left-lateral transtensive faults and rare E–W trending faults were re-activated as transfer faults (e.g. respectively, the Positano-Vettica Maggiore segment of the Scraio-Vettica Maggiore fault zone and the fault bounding the Agerola basin to the S; Fig. 18c). These faults outlined the shape of the peninsula by downfaulting and drowning of the northern and southern blocks (top of carbonates is lowered at 2600–3000 m below the sea level in the adjacent peri-Tyrrhenian grabens). This led to truncation of the II Order paleosurfaces and to collapse of the elevations that had supplied the Agerola breccia and had formed the catchment area of the Nocelle fanglomerates (Fig. 18c).

Coeval to this faulting are the oldest (initial Middle Pleistocene in age) beach deposits resting on the southern slope of the Sorrento peninsula in Conca dei Marini area. These formed along the coastal fault scarps, which in that time had already gained 2/3 of their height, and were subsequently raised at 200–230 m a.s.l. The lack of paleo-sea-level markers at similar elevation in the western portion of the peninsula (W of Positano, the highest and oldest shorelines rest at 23 m a.s.l. and are related to the O.I.S. 9; Cinque and Romano, 1990), and the uneven elevation of shorelines related to the O.I.S. 9, suggest respectively that southward downfaulting and thinning of the ridge along NE–SW trending faults, and differential motions related to faults transverse to the peninsula continued until the mid–late part of the Middle Pleistocene. As a consequence, we conclude that event D3 lasted at least until around 300 ky ago.

During the Early to Middle Pleistocene, the two headlands underwent uplift on the order of some hundreds of metres. In Mt. Bulgheria area, it is recorded by the position of: Santernian marine terraces up to 400 m a.s.l.; Emilian terraces up to 280 m, and Middle Pleistocene shorelines up to 130 m (Fig. 5). In the Sorrento peninsula, it is recorded by the early Middle Pleistocene shore deposits up to 230 m; here uplift was accompanied by an overall gentle tilting (5°–6°) towards the NW, that is recognised by seismic profiles from the Naples Gulf (Milia and Torrente, 1999) and by tilt of the II Order paleosurfaces trend surface.

6.4. Event D4

Event D4 was characterised by an extensional deformation related to a NE–SW trending extension direction, and produced the largest vertical offsets along NW–SE trending faults.

We relate to onset of this tectonic regime the substantial ceasing/slowing down of both differential and absolute vertical motions recorded in the study areas since the late part of the Middle Pleistocene.

During this time span, only negligible displacements are recorded in the study areas. In the Sorrento peninsula, the slight offsets occurred along the NW–SE trending faults transverse to the ridge since 200 ky ago are testified by the O.I.S. 7 markers at a roughly constant elevation, and by the height difference (around 1 m) among the Late Pleistocene shorelines. By comparison of the present elevation of the O.I.S. 7 with the paleoclimatic record (the O.I.S. 7 peak is lower than the Stage 5 one; Lisiecki and Raymo, 2005), a slight uplift of the ridge may be supposed between 200 and 130 ky ago, whereas elevation of O.I.sS. 5e markers testify that this uplift ended since 130 ky. A similar situation is encountered in Mt. Bulgheria area: here only slight vertical differential motion are supposed to have occurred since the late Middle Pleistocene, whereas distribution of O.I.sS. 5e shorelines indicates offsets on the order of few metres (up to about 3 m, by their elevation in Porto Infreschi area; Esposito et al., 2003) since the Late Pleistocene.

7. Discussion

In this chapter, we combine the results of our reconstruction in the study areas with data from other sectors of the Southern Apennines and from the Tyrrhenian offshore, in order to attempt a kinematic reconstruction for the whole Southern Apennines through time.

7.1. Mid–Late Miocene to Pliocene

The results of our study indicate that, during Miocene and Early–Mid-Pliocene, the study areas have been affected by compressional deformation (thrusting, folding and transpressional faulting). According to our data, the orientation of the $\sigma 1$ axis changed from NW–SE of event D1 (during Mid–Late Miocene, until the latest Miocene or earliest Pliocene) to N–S of event D2.

Deformation related to both NW–SE and N–S compressions was recognised in the Sorrento peninsula by Capotorti and Tozzi (1991), that relate the different

compression orientations to "block faulting rotation", and within the whole inner-axial belt of the chain by Hippolyte et al. (1994a) and Hippolyte et al. (1994c). These Authors relate the NW–SE trending compression to minor and local folding and faulting, during a major N–S trending compression active in the Late Miocene–Pliocene, whereas in our case the D1 NW–SE trending compression predates all other events. However, taking into account the recognition by Gattacceca and Speranza (2002) of a 60° counterclockwise rotation in Mt. Bulgheria area during Middle–Late Miocene, we cannot exclude that the present orientation of D1 stress axes resulted from the earliest (pre-rotation) activity of the N–S trending compression of our D2. In the Sorrento peninsula, Tortonian–Early Pliocene activity of a N–S trending compression was recognised also by Milia and Torrente (1999).

To the N–S trending compression, that in the study areas was responsible for major thrust and strike-slip faulting, may be related also the widespread N-verging overthrusts that occur both in the inner belt of the Southern Apennines (Pescatore and Sgrosso, 1973; Ortolani, 1978; Renaud et al., 1990; Ferranti et al., 1996) and in the Tyrrhenian offshore (Bartole et al., 1984).

Event D2 was characterised by an E–W oriented $\sigma 3$ which parallels the central Tyrrhenian basin stretching orientation (Vavilov basin; Sartori, 1990). Hippolyte et al. (1994a) point out the existence of a relation between extension in the Tyrrhenian basin and compression in the chain, the orientation of the maximum horizontal stress remaining the same in both domains. As a consequence, we interpret onset of event D2 as the response, within the Southern Apennines thrust belt, to the stretching that led to opening of the central Tyrrhenian basin. The E–W stretching affected first, in Late Tortonian times, the Sardinia margin to migrate eastwards (Sartori, 1990; Doglioni et al., 2004). Onset, in the study areas, of the dominant extensional deformation related to the late part of event D2, indicates that the present Tyrrhenian margin of the Southern Apennines entered the Tyrrhenian extensional domain starting from the Late Pliocene.

During the Late Pliocene, the thrust belt was still subject to the N–S trending compression (Hippolyte et al., 1994a,c). In our study areas, the ongoing N–S compression is recorded by minor strike-slip deformation coeval to the dominant homoaxial extensional regime. At the same time, some minor E–W trending extensional deformation coeval to the dominant homoaxial N–S oriented compression is recorded within the axial portion of the chain (Ofanto basin; Hippolyte et al., 1994c).

We speculate that to event D2 can be related also several NW–SE trending faults with large horizontal and vertical offsets that are widespread within the whole Tyrrhenian slope of the southern Apennines, from the Campana plain to the Cilento headland (Sartori, 1990; Turco et al., 1990; Ascione et al., 1992a,b; Caiazzo et al., 1992; Cinque et al., 1993; Giordano et al., 1995; Berardi et al., 1996). These large offsets predate formation of widespread Pliocene age paleosurfaces resting at around 1000 m of elevation (Ascione and Cinque, 1999). Within the whole region, there is striking evidence that these paleosurfaces were formed when the inner side of the chain was less elevated and not yet fragmented by peri-Tyrrhenian grabens (Ascione and Cinque, 1999).

7.2. Early to late Middle Pleistocene

Since the Early Pleistocene, is recorded activity of a dominant extensional regime with a NW–SE trending $\sigma 3$ axis (event D3), which created major NE–SW trending normal faults.

A deformational event with the same features of our D3 (i.e. a NW–SE trending extension direction common to a normal and a strike-slip regimes, interrelated through $\sigma 1$–$\sigma 2$ axes permutation), affected also deposits with radiometric age around 650 ky cropping out to the N of the Campana Plain (Prata Sannita basin; Caiazzo et al., 2001). It was also reconstructed in the Sele Plain area and in the axial portion of the Southern Apennines by Hippolyte et al. (1994b) and Hippolyte et al. (1995), who related it to the Early Pleistocene. Early–Middle Pleistocene age extensional tectonics with axis NW–SE was recognised in the Sorrento peninsula also by Milia and Torrente (1999), and to an extensional event responsible for NE–SW trending normal faults Giordano et al. (1995) relate the Pleistocene subsidence of the Garigliano Plain (see Fig. 19 for location).

In the study areas, NW–SE trending left-lateral transtensive faults were active during event D3, and small Early–Middle Pleistocene offsets along NW–SE trending sinistral strike-slip faults are recorded also in Cilento–northern Calabria (Cinque et al., 1993).

Event D3, that outlined the present Sorrento peninsula and Mt. Bulgheria headlands, was also responsible for formation of the series of coastal grabens bounded to the N by major NE–SW trending faults, that characterises the Tyrrhenian margin of the Southern Apennines. The offshore parts of this

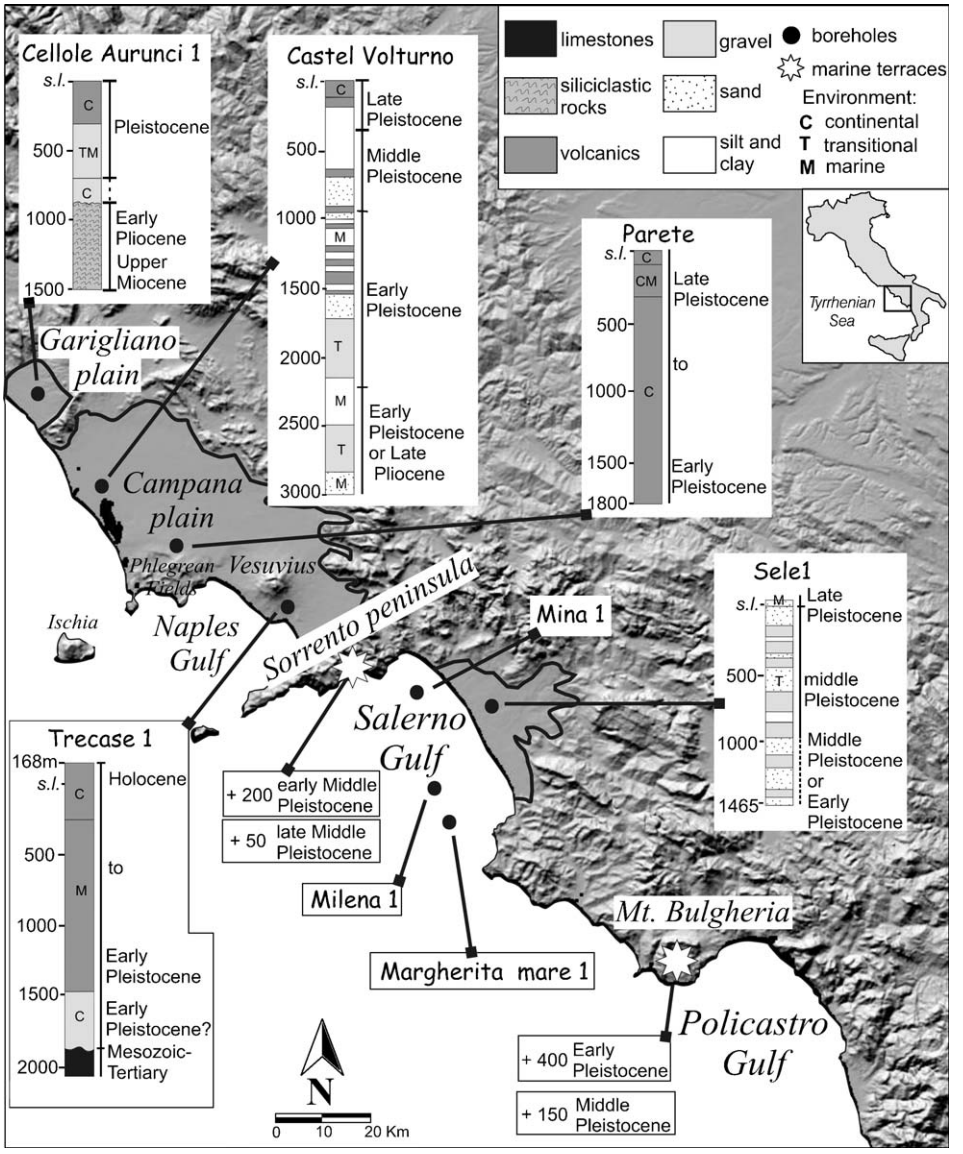

Fig. 19. Elevation of the Lower and Middle Pleistocene shorelines and location of the deepest wells drilled within the peri-Tyrrhenian grabens. Logs are from Ippolito et al. (1973), Brancaccio et al. (1991), and Brocchini et al. (2001).

structure, which are characterised by asymmetric-northward thickening-infillings (Mina 1, Milena 1 and Margherita Mare 1 wells in Sacchi et al., 1994; Fig. 19; seismic profiles in Bartole et al., 1984; Moussat et al., 1986; Mariani and Prato, 1988; Argnani et al., 1989; Bruno et al., 1998; Milia et al., 2003), are interpreted as resulting from NW–SE oriented stretching (Moussat et al., 1986; Rehault et al., 1987; Kastens et al., 1990).

In these peri-Tyrrhenian grabens, severe subsidence (from several hundreds to around 3000 m, with rates up to 2–3 mm/a) took place during the Early and Middle Pleistocene. This is documented by several well data from the coastal plains (Ippolito et al., 1973; Brancaccio et al., 1991; Brocchini et al., 2001; Fig. 19), and in the Salerno graben, also from the offshore (Early Pleistocene age of marine deposits at the depth of around 2000 m in Mina 1 well log; Aiello et al., 1997) and by the sin-rift sediments on land: in the Sele Plain, subsidence was accompanied by deposition (at the toes of the Picentini Mts.; see Fig. 4b for location) of the thick epiclastic Eboli Conglomerates, with radiometric ages ranging from 1.5 to 0.9 Ma (Brancaccio et al., 1991).

This subsidence was coeval to uplift of the interposed horst blocks, as it is documented in the study areas (Section 6.3) and in the Picentini Mts. (Brancaccio et al., 1991) that bound to the N the on land portion of the Salerno Gulf–Sele Plain graben.

End of event D3 in the late Middle Pleistocene is inferred by the marked decrease in rates of activity of the NE–SW trending normal faults along the Tyrrhenian margin. This is recorded by decreasing in both headlands uplift rates (Sections 6.3 and 6.4), and peri-Tyrrhenian grabens subsidence rates, leading to filling up of their present on land portions (Fig. 19). In northern Campana Plain, subsidence rates changed from 2/3 mm/a to 0.75 mm/a (Romano et al., 1994).

The NW–SE trending extension direction active along the Tyrrhenian margin parallels, as already pointed out by Hippolyte et al. (1994a), the stretching orientation which controlled the spreading and deepening in the southeastern Tyrrhenian–Marsili basin — during the Pleistocene (Moussat et al., 1986; Rehault et al., 1987; Sartori, 1990; Savelli and Schreider, 1991).

During this time span, shortening was still ongoing in the outer sectors of the Southern Apennines, where thrusting episodes occurred until the early Middle Pleistocene (around 650 ky; Patacca and Scandone, 2001). This thrusting is referred by Hippolyte et al. (1994c) and Hippolyte et al. (1995) to a compressive tectonic event characterised by a ENE–WSW oriented $\sigma 1$, homoaxial to the extension active in the Tyrrhenian basin. The minor strike-slip regime recorded at the outcrop scale in the study areas during this period may be interpreted as the response to the coeval compression active in the outer portion of the chain.

7.3. Late Middle Pleistocene to Present

The late Quaternary faulting in the Southern Apennines is consistent with the D4 tectonic event, which is characterised by an extensional regime with a NE–SW trending $\sigma 3$ axis. In fact, by the morphostructural, stratigraphic and tectonic data reported in Cinque et al. (2000) (see also references therein), it results that deformation affecting the region in the late Quaternary is represented by mostly NW–SE, subordinately E–W and rarely NE–SW trending faults (Fig. 20). These structures displace depositional landforms, e.g. the slopes of the Roccamonfina volcano and the terraces in the upper valleys of the Volturno and Agri

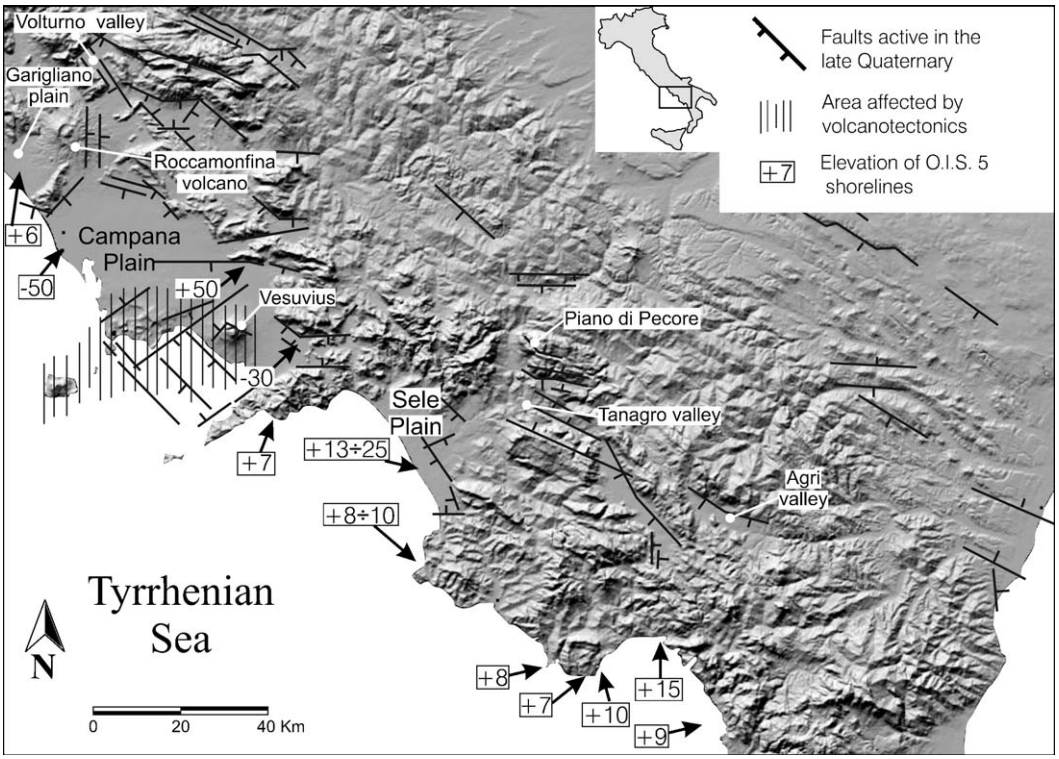

Fig. 20. Faults active in the late Quaternary in the Southern Apennines and elevation of O.I.S. 5 shorelines, mapped onto the DEM of the region. Modified after Cinque et al. (2000).

rivers, the Tanagro river valley and the Sele plain, that are related to the Middle Pleistocene (Amato et al., 1991; Di Niro et al., 1992; De Rita and Giordano, 1996; Brancaccio et al., 1997).

Displacements associated with these faults are generally quite modest, not exceeding few tens of metres. Similar information is obtained from distribution of the Upper Pleistocene to Holocene shore deposits and lines (Fig. 20). These indicate that the Garigliano plain (Brancaccio et al., 1990) and the Sorrento peninsula were substantially stable, whereas a slight uplift affected the northern Cilento headland and the coast of the Policastro Gulf (O.I.S. 5 shorelines respectively ranging from 8 to 10 m a.s.l. and at 15 m a.s.l.; Brancaccio et al., 1990; Cinque et al., 1994), and the Sele Plain (O.I.sS. 5e shorelines at 25 m, and O.I.sS. 5c ones at 13 m a.s.l.; Brancaccio et al., 1987). On the order of few tens of metres is also the subsidence of the Campana Plain, both in its southernmost sector (Brancaccio et al., 1994) and it the northern one: here, the recentmost subsidence and the 50 m uplift of O.I.S. 5 littoral deposits (Romano et al., 1994) is related to the NW–SE trending fault bounding the plain to the east.

Much stronger vertical motions, with average rates up to some cm/yr, affected the central portion of the Campana Plain graben, both offshore (Naples Gulf; Cinque et al., 1997; Milia and Torrente, 1999) and inland (Somma–Vesuvius and Phlegrean Fields volcanic areas; Orsi et al., 1996), and Ischia island (Cinque et al., 1997). However, the vertical motions in these areas were probably related to reactivation of pre-existing faults driven by volcano-tectonic phenomena (Cinque, 1991; Orsi et al., 1996; Cinque et al., 1997).

In almost all cases, the late Quaternary displacements reactivate pre-existing faults. This was observed, for instance, in Mt. Marzano massif (Ascione et al., 2003), where Pliocene age paleosurfaces postdating large fault offsets (both horizontal and vertical), are displaced by recent re-activations of the same faults; among them, the Piano di Pecore one was activated also during the 1980 Irpinia earthquake (Westaway and Jackson, 1987; Pantosti and Valensise, 1990).

Since the NE–SW direction of extension of event D4 parallels to the one obtained, by means of structural and seismological data and by present-day stress measurements also for other sectors of southern Italy (Cello et al., 1982; Gasparini et al., 1985; Westaway and Jackson, 1987; Montone, 1997; Vannucci et al., 2004), we suggest in agreement to Hippolyte et al. (1994b) that this stress field is currently active.

8. Conclusion

The present structural setting of Tyrrhenian slope of the Southern Apennines results from a succession of first compressional, and subsequently extensional tectonic events, which took place from Mid–Late Miocene to the Present.

The compressional tectonics, first NW-verging (event D1) and subsequently N-verging (event D2), reflects the major convergence of Africa to Europe. In this frame, event D1 (active since Mid–Late Miocene) may be regarded as predating the late Tortonian onset of the Tyrrhenian extension, or/and as occurred when the eastwards migrating Tyrrhenian extension had not yet reached the present inner slope of the chain.

The N-vergent compression of event D2, which started in late Miocene or earliest Pliocene and was characterised by an E–W oriented $\sigma 3$ axis, was coeval to the stretching in the central Tyrrhenian extensional basin. Subsequently (i.e. in the Late Pliocene), while the N-verging compression was still active in the Southern Apennines, the inner side of the chain entered the Tyrrhenian extensional domain. In this side of the chain, event D2 was in this period dominated by an extensional regime, the $\sigma 3$ axis being oriented E–W, homoaxial to the formerly dominating N–S compression.

Structures created by event D2 have undergone severe erosion/planation during the Pliocene, when several paleosurfaces developed in the region (Ascione and Cinque, 1999). The elevations up to 800–1000 m high surrounding the Upper Pliocene Camerota basin (Section 4.1) testify that, during this period, the inner side of the chain had already suffered some uplift, most probably in response to thrusting.

In the Early Pleistocene (event D3), the minimum stress orientation changed to NW–SE both in the Tyrrhenian basin and in the chain. During this period, shortening was active in the outer belt of the chain with an ENE–WSW trending compression, which is related by Hippolyte et al. (1994a) to the N–S convergence of Europe and Africa in a complex pattern of blocks and arcs. The change in the basin extension direction may be related, according to Doglioni et al. (1994), to the encroachment of the Adriatic thick continental lithosphere E of the Southern Apennines, which slowed that segment of the subduction, whereas the roll-back concentrated to the SE towards the Ionian oceanic lithosphere (Doglioni et al., 2004).

During this period, the Tyrrhenian margin of the chain was affected by a dominant extension, that created a major horst-and-graben structure with a NE–SW trend. While the peri-Tyrrhenian grabens suffered strong

subsidence, the horst structures underwent uplift that may be principally related to rift flank uplift. However, as in Quaternary times the whole chain was affected by some uplift (although with a less amount in the Tyrrhenian side than in the outer one; Cinque et al., 1993; Amato and Cinque, 1999; Ascione and Cinque, 1999) the contribution of a long-wavelength uplift component may be envisaged. This component may be referred to isostatic rebound probably related, following Doglioni et al. (2003) and Doglioni et al. (2004), to the underlying eastward transit of a depleted and less dense astenosphere.

In response to the Early–Middle Pleistocene vertical faulting and uplift, but also to downcutting by rivers flowing towards the newborn Tyrrhenian coast, a strong increase in the local relief took place in the whole Tyrrhenian slope of the chain. Due to dissection, large volumes of the widespread soft siliciclastic covers (e.g. Miocene flysch, internal nappes) were dismantled, leading to the development of several high fault line scarps along pre-existing fault planes, most of them created during event D2.

Since the late Middle Pleistocene, onset of the extensional event D4 is recorded. According to Hippolyte et al. (1994b), the NE-trending extension marks a major geodynamical change with the cessation of the compression–extension couple of deformation in the chain and in the southern Tyrrhenian basin.

Event D4, which is currently active, has only slightly modified the morphotectonic signature (i.e. topographic highs and lows created by tectonic/erosional processes) developed during event D3. The moderate surface expression of this recent faulting is not only due to its young age, but also to the overall low rates of activity of single faults (Cinque et al., 2000).

Acknowledgments

We wish to thank Prof. Giuseppe Cello, Dr. Jean-Claude Hippolyte, Dr. Liviu Matenco and an anonymous referee for their constructive suggestions, which helped us to improve the manuscript.

References

Aiello, G., Budillon, F., de Alteris, G., Di Razza, O., De Lauro, M., Ferraro, L., Marsella, E., Pelosi, N., Pepe, F., Sacchi, M., Tondelli, R., 1997. Seismic exploration of the peri-Tyrrhenian basins in the Latium–Campania offshore. 8th Workshop of the ILP Task Force "Origin of Sedimentary Basins", Palermo (Italy), 7–13 June 1997, pp. 22–23.

Amato, A., Cinque, A., 1999. The erosional landsurfaces of the Campano–Lucano Apennines (S. Italy): genesis, evolution and tectonic implications. Tectonophysics 315, 251–267.

Amato, A., Robustelli, G., 2002. The Nocelle conglomerates: a problematic outcrop highly suspended on the southern slope of the eastern Sorrento peninsula (Italy). Il Quaternario 15 (1), 83–96.

Amato, A., Ascione, A., Cinque, A., Lama, A., 1991. Morfoevoluzione, sedimentazione e tettonica recente dell'alta Piana del Sele e delle sue valli tributarie. Geogr. Fis. Din. Quat. 14, 5–16.

Amore, F.O., Bonardi, G., Ciampo, G., de Capoa, P., Perrone, V., Sgrosso, I., 1988. Relazioni tra "flysch interni" e domini appenninici: reinterpretazione delle formazioni di Pollica, San Mauro e Albidona e il problema dell'evoluzione inframiocenica delle zone esterne appenniniche. Mem. Soc. Geol. Ital. 41, 285–297.

Angelier, J., 1994. Fault slip analysis and paleostress reconstruction. In: Hancock, P.L. (Ed.), Continental Deformation. Pergamon Press, Oxford, pp. 53–100.

Angelier, J., Bergerat, F., 1983. Systèmes de contrainte et extension intracontinentale. Bull. Cent. Rech. Explor. Prod. Elf-Aquitaine 7, 137–147.

Argnani, A., Bortoluzzi, G., Bozzani, A., Canepa, A., Ligi, M., Palumbo, V., Serracca, P., Trincardi, F., 1989. Sedimentary dynamics on the Eastern Tyrrhenian Margin, Italy. PS/87 Cruise report. G. Geol. III (51/1), 165–178.

Armijo, R., Cisternas, A., 1978. Un probléme inverse en microtectonique cassante. C. R. Acad. Sci. Paris, Terre 287, 595–598.

Ascione, A., Cinque, A., 1999. Tectonics and erosion in the long term relief history of the Southern Apennines (Italy). Z. Geomorphol., Suppl.Bd 118, 1–16.

Ascione, A., Romano, P., 1999. Vertical movements on the eastern margin of the Tyrrhenian extensional basin. New data from Mt. Bulgheria (Southern Apennines, Italy). Tectonophysics 315, 337–356.

Ascione, A., Cinque, A., Santangelo, N., Tozzi, M., 1992a. Il bacino del Vallo di Diano e la tettonica trascorrente plio-quaternaria: nuovi vincoli cronologici e cinematici. Studi Geolog. Camerti, Vol. Spec. 1992/1, 209–219.

Ascione, A., Cinque, A., Tozzi, M., 1992b. La Valle del Tanagro (Campania): una depressione strutturale ad evoluzione complessa. Studi Geolog. Camerti, Vol. Spec. 1992/1, 201–208.

Ascione, A., Caiazzo, C., Hippolyte, J.-C., Romano, P., 1997. Pliocene–Quaternary extensional tectonics and morphogenesis at the eastern margin of the southern Tyrrhenian basin (Mt. Bulgheria, Campania region, Italy). Il Quaternario 10 (2), 571–578.

Ascione, A., Cinque, A., Improta, L., Villani, F., 2003. Late Quaternary faulting within the Southern Apennines seismic belt: new data from Mt. Marzano area (Southern Apennines). Quat. Int. 101–102, 27–41.

Bartole, R., Savelli, D., Tramontana, M., Wezel, F.C., 1984. Structural and sedimentary features in the Tyrrhenian margin off Campania, southern Italy. Mar. Geol. 55 (2/2), 163–180.

Berardi, F., De Rosa, G., Tozzi, M., 1996. Vincoli strutturali di superficie per una ricostruzione geometrica del massiccio dei Monti Alburni (Appennino meridionale). Mem. Soc. Geol. Ital. 11, 201–216.

Bigi, G., Coli, M., Cosentino, D., Parotto, M., Praturlon, A., Sartori, R., Scandone, P., Turco, E. (Eds.), 1983. Structural Model of Italy. C.N.R., Progetto Finalizzato Geodinamica, Roma.

Bonaduce, G., Ruggieri, G., Russo, A., 1987. The ostracode genus *Mutulus* and some so-called Mutulus from the Mediterranean Miocene–Pleistocene. Boll. Soc. Paleontol. Ital. 26 (3), 251–268.

Borrelli, A., Ciampo, G., De Falco, M., Guida, D., Guida, M., 1988. La morfogenesi del M. Bulgheria (Campania) durante il Pleistocene inferiore e medio. Mem. Soc. Geol. Ital. 41, 667–672.

Brancaccio, L., Capaldi, G., Cinque, A., Pece, R., Sgrosso, I., 1978. Th/U dating of corals from a Tyrrhenian beach in Sorrentine Peninsula (southern Italy). Quaternaria 20, 175–183.

Brancaccio, L., Cinque, A., D'Angelo, G., Russo, F., Santangelo, N., Sgrosso, I., 1987. Evoluzione tettonica e geomorfologica della Piana del Sele (Campania, Appennino meridionale). Geogr. Fis. Din. Quat. 10, 47–55.

Brancaccio, L., Cinque, A., Russo, F., Belluomini, G., Branca, M., Delitala, L., 1990. Segnalazione e datazione di depositi marini tirreniani della costa campana. Boll. Soc. Geol. Ital. 109, 259–265.

Brancaccio, L., Cinque, A., Romano, P., Rosskopf, C., Russo, F., Santangelo, N., Santo, A., 1991. Geomorphology and neotectonic evolution of a sector of the Tyrrhenian flank of the Southern Apennines (Region of Naples, Italy). Z. Geomorphol., Suppl.Bd 82, 47–58.

Brancaccio, L., Fiume, G., Grimaldi, M., Rapolla, A., Romano, P., 1994. Analisi gravimetriche nella bassa valle del torrente Solofrana (SA) e considerazioni sulla sua evoluzione quaternaria. Il Quaternario 117 (2), 131–138.

Brancaccio, L., Cinque, A., Di Crescenzo, G., Santangelo, N., Scarciglia, F., 1997. Alcune osservazioni sulla tettonica quaternaria nell'alta valle del F. Volturno. Il Quaternario 10 (2), 321–328.

Brocchini, D., Principe, C., Castradori, D., Laurenzi, M.A., Gorla, L., 2001. Quaternary evolution of the southern sector of the Campana Plain and early Somma–Vesuvius activity: insight from the Trecase 1 well. Mineral. Petrol. 73, 67–91.

Bruno, P.P.G., Cippitelli, G., Rapolla, A., 1998. Seismic study of the Mesozoic carbonate basement around Mt. Somma–Vesuvius, Italy. J. Volcanol. Geotherm. Res. 84, 311–322.

Caiazzo, C., Giovine, G., Ortolani, F., Pagliuca, S., Schiattarella, M., Vitale, C., 1992. Genesi ed evoluzione strutturale della depressione tettonica dell'alta valle del fiume Sele (Appennino campano-lucano). Studi Geolog. Camerti, Vol. Spec. 1992/1, 245–255.

Caiazzo, C., Cinque, A., Merola, D., 2000. Relative chronology and kinematics of the Apenninic and anti-Apenninic faults in the Sorrento peninsula. Mem. Soc. Geol. Ital. 55, 165–174.

Caiazzo, C., Ruggieri, G., Morra, V., Santangelo, N., Villa, I., 2001. Quaternary evolution of the Prata Sannita basin (southern Italy): morphostructural, microtectonic and radiometric analysis. Int. Workshop "Uplift and Erosion: Driving Processes and Resulting Landforms", Siena (Italy), 20–21 Sept. 2001, p. 23.

Capotorti, F., Tozzi, M., 1991. Tettonica trascorrente nella penisola sorrentina. Mem. Soc. Geol. Ital. 47, 235–249.

Cello, G., Mazzoli, S., 1999. Apennine tectonics in southern Italy: a review. J. Geodyn. 27, 191–211.

Cello, G., Guerra, I., Tortorici, L., Turco, E., Scarpa, R., 1982. Geometry of the neotectonic stress field in southern Italy: geological and seismological evidence. J. Struct. Geol. 4, 385–393.

Cello, G., Lentini, F., Tortorici, L., 1990. La struttura del settore calabro-lucano e suo significato nel quadro dell'evoluzione tettonica del sistema a thrust sudappenninico. Studi Geol. Camerti 1990, 27–34.

Ciampo, G., 1976. Ostracodi pleistocenici di Cala Bianca (Marina di Camerota, Salerno). Boll. Soc. Paleontol. Ital. 15, 3–23.

Cinque, A., 1991. La trasgressione versiliana nella Piana del Samo (Campania). Geogr. Fis. Din. Quat. 14, 63–71.

Cinque, A., Romano, P., 1990. Segnalazione di nuove evidenze di antiche linee di riva in Penisola Sorrentina (Campania). Geogr. Fis. Din. Quat. 13 (1), 23–36.

Cinque, A., Patacca, E., Scandone, P., Tozzi, M., 1993. Quaternary kinematic evolution of the Southern Apennines. Relationship between surface geological features and deep lithospheric structures. Ann. Geofis. 36 (2), 249–260.

Cinque, A., Romano, P., Rosskopf, C., Santangelo, N., Santo, A., 1994. Morfologie costiere e depositi quaternari tra Agropoli e Ogliastro Marina (Cilento, Italia meridionale). Il Quaternario 7 (1), 3–16.

Cinque, A., Aucelli, P.P.C., Brancaccio, L., Mele, R., Milia, A., Robustelli, G., Romano, P., Russo, F., Santangelo, N., Sgambati, D., 1997. Volcanism tectonics and recent geomorphological change in the bay of Napoli. IV Int. Conf. on Geomorph. Geogr. Fis. Din. Quat., Suppl., vol. III-t.2, pp. 123–141. Guide for Excursion.

Cinque, A., Ascione, A., Caiazzo, C., 2000. Distribuzione spazio-temporale e caratterizzazione della fagliazione quaternaria in Appennino Meridionale. In: Galadini, F., Meletti, C., Rebez, A. (Eds.), Ricerche del GNDT nel campo della pericolosità sismica (1996–1999). CNR-GNDT Spec. Publ. Roma, pp. 203–218.

De Blasio, I., Lima, A., Perrone, V., Russo, M., 1981. Nuove vedute sui depositi miocenici della Penisola Sorrentina. Boll. Soc. Geol. Ital. 100, 57–70.

de Kaenel, E., Siesser, W.G., Murat, A., 1999. Pleistocene calcareous nannofossils biostratigraphy and the western Mediterranean sapropels, Sites 974 to 977 and 979. In: Zahn, R., Comas, M.C., Klaus, A. (Eds.), Proceedings of ODP. Scientific Results, vol. 161. Ocean Drilling Program, College Station, TX, pp. 159–183.

De Rita, D., Giordano, G., 1996. Volcanological and structural evolution of Roccamonfina volcano (southern Italy) and structural origin of the summit caldera. In: Mc Guire, W.J., Jones, A.P., Neuberg, J. (Eds.), Volcano Instability on Earth and Other Planets. Geol. Soc. Am., Spec. Publ., vol. 110, pp. 209–224.

Di Niro, A., Giano, S.I., Santangelo, N., 1992. Primi dati sull'evoluzione geomorfologica e sedimentaria del bacino dell'alta Val d'Agri. Studi Geolog. Camerti, Vol. Spec. 1992/1, 257–263.

Doglioni, C., Mongelli, F., Pieri, P., 1994. The Puglia uplift (SE Italy): an anomaly in the foreland of Apenninic subduction due to buckling of a thick continental lithosphere. Tectonics 13, 1309–1321.

Doglioni, C., Carminati, E., Bonatti, E., 2003. Rift asymmetry and continental uplift. Tectonics 22 (3), 1024, doi:10.1029/2002TC001459.

Doglioni, C., Innocenti, F., Morellato, C., Procaccianti, D., Scrocca, D., 2004. On the Tyrrhenian sea opening. Mem. Descr. Carta Geol. Ital. 44, 147–164.

Esposito, C., Filocamo, F., Marciano, R., Romano, P., Santangelo, N., Scarciglia, F., Tuccimei, P., 2003. Late Quaternary shorelines in southern Cilento (Mt. Bulgheria): morphostratigraphy and chronology. Il Quaternario 16 (1), 3–14.

Etchecopard, A., Vasseur, G., Daignieres, M., 1981. An inverse problem in microtectonics for the determination of stress tensors from fault striation analysis. J. Struct. Geol. 3, 51–65.

Ferranti, L., Oldow, J.S., Sacchi, M., 1996. Pre-Quaternary orogen-parallel extension in Southern Apennines belt, Italy. Tectonophysics 260, 325–347.

Gasparini, C., Iannaccone, G., Scarpa, R., 1985. Fault-plane solution and seismicity of the Italian Peninsula. Tectonophysics 117, 59–78.

Gattacceca, J., Speranza, F., 2002. Paleomagnetism of Jurassic to Miocene sediments from the Apenninic carbonate platform

(southern Apennines, Italy): evidence for a 60° counterclockwise Miocene rotation. Earth Planet. Sci. Lett. 201, 19–34.

Giordano, G., Naso, G., Trigari, A., 1995. Evoluzione tettonica di un settore particolare del margine tirrenico: l'area al confine tra Lazio e Campania, prime considerazioni. Studi Geolog. Camerti, Vol. spec. 1995/2, 269–278.

Hippolyte, J.-C., 2001. Paleostress and neotectonic analysis of sheared conglomerates: Southwest Alps and Southern Apennines. J. Struct. Geol. 23, 421–429.

Hippolyte, J.-C., Angelier, J., Roure, F., 1994a. Paleostress analyses and fold-and-thrust belt kinematics in the Southern Apennines. In: Roure, F., Ellouz, N., Shein, V.S., Skvortsov, I. (Eds.), Proceedings of The International Symposium "Geodynamic Evolution Of Sedimentary Basins", Moscow, 1992. Éditions Technip, Paris, pp. 157–169.

Hippolyte, J.-C., Angelier, J., Roure, F., 1994b. A major geodynamic change revealed by Quaternary stress patterns in the Southern Apennines (Italy). Tectonophysics 230, 199–210.

Hippolyte, J.-C., Angelier, J., Roure, F., Casero, P., 1994c. Piggyback basin development and thrust belt evolution: structural and paleostress analyses of Plio-Quaternary basins in the Southern Apennines. J. Struct. Geol. 16, 159–173.

Hippolyte, J.-C., Angelier, J., Barrier, E., 1995. Compressional and extensional tectonics in an arc system: example of the Southern Apennines. J. Struct. Geol. 17 (12), 1725–1740.

Ippolito, F., Ortolani, F., Russo, M., 1973. Struttura marginale tirrenica dell'Appennino campano: reinterpretazione di dati di antiche ricerche di idrocarburi. Mem. Soc. Geol. Ital. 12, 227–250.

Kastens, K., Mascle, J., ODP Leg 107 Scientific Party, 1990. Proceedings of Ocean Drilling Program, Scientific Results, vol. 107. Ocean Drilling Program, College Station, TX.

Lambeck, K., Chappell, J., 2001. Sea level change during the Last Glacial cycle. Science 292, 679–686.

Lippmann-Provansal, M., 1987. L'Apennin Campanien Mèridional (Italie). Etude Geomorphologique. These de Doctorat, Università Aix-Marseille, Aix en Provence.

Lisiecki, L., Raymo, M., 2005. A Pliocene–Pleistocene stack of 57 globally distributed benthic $\delta^{18}O$ records. Paleoceanography 20, A1003, doi:10.1029/2004PA001071.

Malinverno, A., Ryan, W.B.F., 1986. Extension in the Tyrrhenian sea and shortening in the Apennines as result of arc migration driven by sinking in the lithosphere. Tectonics 5 (2), 227–245.

Mariani, M., Prato, R., 1988. I bacini neogenici costieri del margine tirrenico: approccio sismico-stratigrafico. Mem. Soc. Geol. Ital. 41, 519–531.

Milia, A., Torrente, M.M., 1999. Tectonics and stratigraphic architecture of a peri-Tyrrhenian half-graben (Bay of Naples, Italy). Tectonophysics 315, 301–318.

Milia, A., Torrente, M.M., Russo, M., Zuppetta, A., 2003. Tectonics and crustal structure of the Campania continental margin: relationships with volcanism. Mineral. Petrol. 79, 33–47.

Montone, P., 1997. The active crustal stress: methods and results in Italy. Il Quaternario 10 (2), 313–320.

Moussat, E., Rehault, J.P., Fabbri, A., 1986. Rifting et èvolution tectono-sèdimentaire du Bassin Tyrrhènien au cours du Neogene et du Quaternaire. G. Geol. ser. 3, 48 (1/2), 41–62.

Orsi, G., de Vita, S., Di Vivo, M., 1996. The restless, resurgent Campi Flegrei nested caldera (Italy): constraints on its evolution and configuration. J. Volcanol. Geotherm. Res. 74, 179–214.

Ortolani, F., 1978. Alcune considerazioni sulle fasi tettoniche mioceniche e plioceniche dell'Appennino meridionale. Boll. Soc. Geol. Ital. 97, 609–616.

Pantosti, D., Valensise, G., 1990. Faulting mechanisms and complexity of the November 23, 1980, Campania — Lucania earthquake, inferred from surface observations. J. Geophys. Res. 95 (B10), 15.319–15.341.

Pasini, G., Colalongo, M.L., 1994. Proposal for the erection of the Santernian/Emilian boundary stratotype (lower Pleistocene) and new data on the Pliocene/Pleistocene boundary stratotype. Boll. Soc. Paleontol. Ital. 33 (1), 101–120.

Patacca, E., Scandone, P., 2001. Late thrust propagation and sedimentary response in the thrust belt-foredeep system in the Southern Apennines (Pliocene–Pleistocene). In: Vai, G.B., Martini, I.P. (Eds.), Anatomy of an Orogen. Kluwer Academic Publishers, London, pp. 401–440.

Patacca, E., Sartori, R., Scandone, P., 1990. Thyrrenian basin and Apenninic arcs: kinematic relations since Late Tortonian times. Mem. Soc. Geol. Ital. 45, 425–451.

Pescatore, T., Sgrosso, I., 1973. I rapporti tra la piattaforma campano-lucana e la piattaforma abruzzese-campana nel casertano. Boll. Soc. Geol. Ital. 92, 597–608.

Rehault, P., Moussat, E., Fabbri, A., 1987. Structural evolution of the Tyrrhenian back-arc basin. Mar. Geol. 74, 123–150.

Renaud, P., Billaud, Y., Clermontè, J., Lorenz, C., Pironon, B., 1990. Evolution paléogéographique le long de la bordure sud orientale de la plate-forme campano-abruzzaise (Italie) du Crétacea u Neogène. Boll. Soc. Geol. Fr. 8, 105–112.

Riccio, A., Riggio, F., Romano, P., 2001. Sea level fluctuations during Oxygen Isotope Stage 5: new data from fossil shorelines in the Sorrento Peninsula (southern Italy). Z. Geomorphol. 45 (1), 121–137.

Romano, P., Santo, A., Voltaggio, M., 1994. L'evoluzione geomorfologica della piana del fiume Volturno (Campania) durante il tardo Quaternario (Pleistocene medio-superiore — Olocene). Il Quaternario 7 (1), 41–56.

Russo, F., 1994. Segnalazione di un livello fossilifero riferibile al Tirreniano a Cala Bianca (Marina di Camerota, Salerno). Mem. Descr. Carta Geol. Ital. 52, 395–398.

Russo Ermolli, E., 1999. Vegetation dynamics and climate changes at Camerota (Campania, Italy) at the Plio-Pleistocene boundary. Il Quaternario 12 (2), 207–214.

Sacchi, M., Infuso, S., Marsella, E., 1994. Late Pliocene–Early Pleistocene compressional tectonics in offshore Campania (Eastern Tyrrhenian Sea). Boll. Geofis. Teor. Appl. 36 (141/144), 469–482.

Sartori, R., 1990. The main results of ODP Leg 107 in the frame of Neogene to Recent geology of the Peri-Tyrrhenian areas. In: Kastens, A., Mascle, K.J., et al. (Eds.), Proceedings of ODP, Scientific Results, vol. 107. Ocean Drilling Program, College Station, TX, pp. 715–730.

Savelli, C., Schreider, A.A., 1991. The opening processes in the deep Tyrrhenian basins of Marsili and Vavilov, as deduced from magnetic and chronological evidence of their igneous crust. Tectonophysics 190, 119–131.

Scandone, P., Sgrosso, I., Bruno, F., 1963. Appunti di geologia sul Monte Bulgheria (Salerno). Boll. Soc. Nat. Napoli 72, 125–131.

Shackleton, N.J., Opdike, N.D., 1973. Oxygen isotope and paleomagnetic stratigraphy of the equatorial Pacific core V28-238: oxygen isotope temperatures and ice volumes on a 10^5 years and 10^6 years scale. Quat. Res. 3, 39–55.

Tozzi, M., Menconi, A., Sciamanna, S., 1996. Studio strutturale del M. Bulgheria (Cilento meridionale) e sue implicazioni per la tettogenesi dell'Appennino campano. Boll. Soc. Geol. Ital. 115, 249–278.

Turco, E., Maresca, R., Cappadona, P., 1990. La tettonica plio-pleistocenica del confine calabro-lucano: modello cinematico. Mem. Soc. Geol. Ital. 45, 519–529.

Ulzega, A., Hearty, P.J., 1986. Geomorphology, stratigraphy and geochronology of Late Quaternary marine deposits in Sardinia. Z. Geomorphol. N.F. Suppl. 62, 119–129.

Vannucci, G., Pondrelli, S., Argnani, A., Morelli, A., Gasperini, P., Boschi, E., 2004. An atlas of Mediterranean seismicity. Ann. Geophys. 47 (1), 247–306 (suppl. to Vol.).

Westaway, R., Jackson, J.A., 1987. The earthquake of 1980 November 23 in Campania–Basilicata (southern Italy). Geophys. J. R. Astron. Soc. 90, 375–443.